Instability of a user equilibrium traffic assignment integrated with a detailed intersection capacity analysis

Master thesis

C. (Chiel) M.S. van der Ster

Internal committee members
Dr. A. Tirachini
Prof. Dr. Ir. E. C. van Berkum

External committee members
Ir. R. Dolman
Dr. Ir. G. Tamminga

Department of Civil Engineering
University of Twente

June 18, 2024

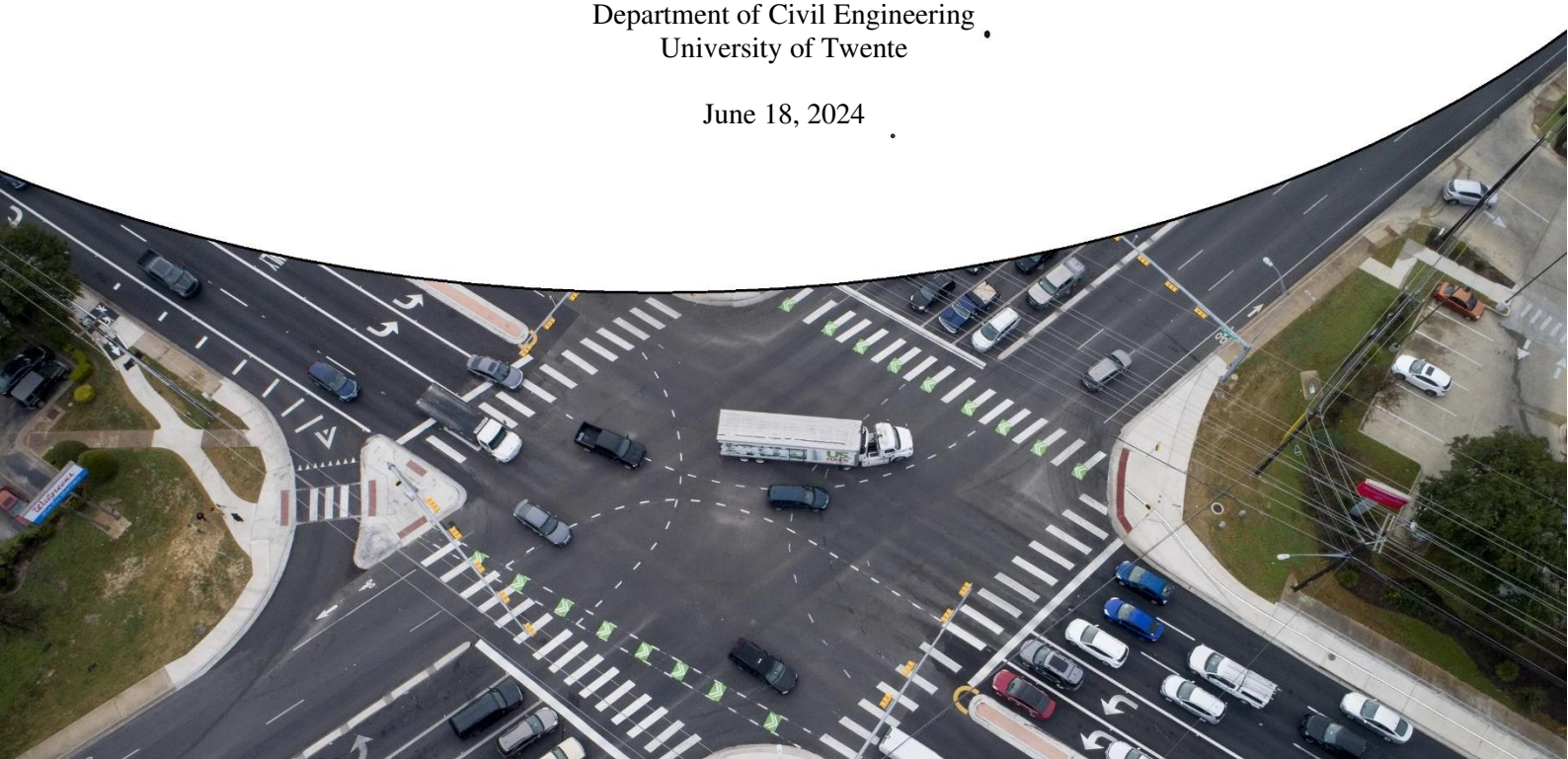

Preface

With this thesis as the final product of my master Civil Engineering and Management, my time at the University of Twente ends. During my years in the bachelor's and master's, it was a pleasure being a student and learning about all concepts in the field of Civil Engineering. In the past 9 months, I had the opportunity to learn more about the application of traffic assignments in traffic models. This would not be possible without the consultancy company Sweco, which offered me this graduation assignment. I hope that the delivery of this thesis has contributed to the encountered issues, and supports Sweco in their projects in the future. Additionally, I want to express my gratitude to the people who supported me through the process of writing this master thesis.

First, I want to thank my daily supervisor at Sweco, Roemer Dolman, for his supervision during this thesis. Roemer has always adopted an enthusiastic and open attitude during my time at Sweco. Additionally, with his analytical and critical thinking, the meetings we had were always enjoyable and of great value. I also want to thank Guus Tamminga, for his inspiring ideas and guidance during the proposal of this thesis. Lastly, my thanks go to Martijn van Rij, the manager of the team "Modellen en Data" in which I had the privilege to work.

Second, I would like to thank my daily supervisor at the university, Alejandro Tirachini, for the meetings we had and his critical view on the topic. This helped a lot in meeting the scientific standards of both the content as well as the report. Furthermore, I want to thank Eric van Berkum for his supervision as coordinator of this thesis. Eric has shown his interest in the topic and made sure the research kept going in the right direction.

With this, I would like to end and I hope you have an enjoyable experience reading my thesis.

Chiel van der Ster

Enschede, June 18, 2024

Abstract

The application of traffic models has become more structural due to the urbanization growth of cities worldwide. In traffic models, a traffic situation is predicted by solving an equilibrium, a state in which no driver can improve its route anymore. Many algorithms have been developed to improve the quality of equilibria, to the reality more precisely. Recent developments have combined the traditional equilibrium-solving process with the detailed Intersection Capacity Analysis (ICA) (TRB, 2016). This together has been realized as the ICA assignment, an iterative procedure promising to deliver a high level of detail in the prediction of traffic flows. However, the ICA assignment is established to be unstable. It has a strong response to very small input perturbations which jeopardizes solutions reliability.

This study aims to examine the instability causes of the ICA assignment and identify the impact of its parameters on the stability. Three types of equilibrium-solving algorithms, the balancing equilibrium assignment (BEA), the Bi-Conjugate Frank Wolfe (BFW), and Linear User Cost Equilibrium (LUCE) are proposed and compared within the ICA assignment.

Stability is defined as the difference in link-flows when demand in a single OD-pair is perturbed with a small value. An assessment framework measures stability as the changed proportion of links, the average and maximum relative error. At first, the stability is investigated in a small case study, the elementary network. In this network, vehicles travel across two intersections calculated with ICA. To enhance its value, a second case study is carried out in a real-world network located in the municipality of Utrecht, the Netherlands. Here, 23 intersections were used for the calculation with ICA. In both networks, 7 distinct parameters have been analyzed by setting up and executing experiments.

The analysis in the elementary network yields that instability shows up when congestion occurs. In the congested phase, the ICA assignment is not able to converge to a single optimal solution and oscillates between multiple solutions. It has been found that the queuing around the intersections calculated with ICA primarily causes this oscillating behavior. No significant differences have been found between the different equilibrium algorithms. In the real-world network, the ICA assignment with BFW was shown to be very unstable. The BEA is found to be the most stable algorithm, although its equilibrium is composed of very few alternative routes compared to the BFW. As a result, adopting a stable equilibrium assignment is likely to give an underestimate prediction of reality. In general, lowering the maximum gap of the equilibrium algorithms leads to improved stability of the ICA assignment, while maintaining the overall accuracy of the equilibrium assignments.

Comparing different configurations of calculated intersections with the ICA confirms the congestion influence on the instability of the ICA assignment. The ICA intersections that are unable to handle all traffic volumes are found to be the major cause of the instability. Hence, equipping more intersections with the ICA will lead to more instability of the ICA assignment as well.

Table of Contents

Table of Figures

Table of Tables

1 Introduction

1.1 Background

The ongoing process of urban development entails complexities in traffic management systems. Because of the growing population in the world, city expansion is inevitable and involves strategic urban planning, infrastructure development, and sustainable resource management. This expansion includes the development of different land-use areas such as neighborhoods, commercial zones, and industry. Between these areas, there is a high rate of transportation activities consisting of people movements and distribution of goods and services. A proper infrastructure network including roads, highways, and public transit systems is essential to avoid moving vehicles ending up in severe congestion. With the growth of urban areas, these congestion challenges are faced much more often.

Transportation engineers and planners use traffic models to predict the movements of traffic such that congestion, pollution, and accessibility can be identified (Ortúzar & Willumsen, 2011). Using data such as traffic counts, vehicle types, and travel patterns, these models can replicate the complex interactions between drivers, vehicles, pedestrians, and the physical road infrastructure. With the ability to demonstrate the effects of new infrastructure implementations, traffic models can be applied to assess potential solutions before executing them in the real world.

In traffic models, traffic flows are predicted by carrying out a traffic assignment. A traffic assignment allocates a given set of trips to a specific transport network (Patriksson, 2015). This allocation is done under the assumption that all travelers are trying to minimize their travel costs. As a result, the traffic will reach a state of equilibrium where no single driver can reduce their travel costs by switching routes — a concept known as the Wardrop equilibrium (Wardrop, 1952). Next to the estimation of traffic volumes, the travel times or road costs are returned too. These types of traffic assignments are static as traffic changes over time are not considered. Travelers' route choices are deterministic because they all agree on the available shortest routes and travel times in the network. Static deterministic traffic assignments are mainly applied for long-term planning objectives where the demand is relatively stable.

Beckman et al (1956) found that specific circumstances cause the Wardrop equilibrium resulting from a traffic assignment to be unique. A unique equilibrium is desired, because multiple equilibriums burden the choice of picking the ‘right’ one that describes reality best. For a unique equilibrium, a slight change in the given traffic situation returns a new unique equilibrium but must conform to a similar equilibrium as the former situation. In the case of a different equilibrium, the traffic assignment is unstable and is a common phenomenon seen in variants of traffic assignments (Beckman et al., 1956). A traffic assignment must be stable for comparison and delivery of trustworthy results. However, the number of studies that research the problem of instability in static traffic assignments is limited. Moreover, the definitions of stability of traffic assignments in executed research vary. Besides Beckmann (1956), Smith (1979) and Jin (2008) defined stability in the context of static deterministic equilibria as asymptotic: an arbitrary initial traffic state close to an equilibrium will converge to it. Nie (2010) uses the model response to a small input perturbation as a measure of stability. This perturbation is a small number of travelers that switch routes. The model is then stable if the equilibrium stays the same. Lu & Nie (2010) mention stability as a sensitivity measure. A stable equilibrium is robust and small perturbations should lead to a slightly different equilibrium. The definition of Lu & Nie (2010) is more accessible and measurable. Therefore, this definition of stability is taken as a directory in this study.

An important factor influencing the traveler's route choice is places of conflict. Traffic conflicts occur at intersections, locations where three or more roads come together. To maintain the safety of travelers, appropriate intersection designs are necessary.

With the correct design, the throughput can be optimized under safe circumstances. Intersections are divided into two main categories: unsignalized or signalized. Among the unsignalized intersections, three subcategories are distinguished: uncontrolled, priority, and roundabout. The selection of the

appropriate control for an intersection is made based on standards and guidance from governmental organizations (Federal Highway Administration, 2023) (National Research Council (U.S.). Transportation Research Board., 2022) (CROW, 2015). Safety, mobility, and geometry are the most important factors for the determination of intersection control. Signalized intersections have been proven effective in reducing the severity of crashes as traffic is regulated in a structured manner (National Highway Traffic Safety Administration (NHTSA), 2003). Crashes at intersections are more likely to occur when a higher traffic flow is expected. Therefore, signalized intersections are often chosen at locations where high volumes meet each other. The regulation at signalized intersections consists of phases in which green is given to lanes that do not conflict with each other. Because a signalized intersection cannot give green to all turns at once, it will increase travel times for many routes. Especially at intersections with high volumes, queues emerge while vehicles wait for green. Overall, intersections play a significant role in the route choice and hence the outcome of a traffic assignment.

Due to recent developments in intersection analysis in transport modeling, the stability of traffic assignments is further tested. In standard traffic assignments, travel time at intersections is determined as a fixed value. An improvement on this is incorporated by more advanced models, which use a different value depending on the turn that is traveled. However, the actual delay encountered by each direction at an intersection is still underestimated. To accurately estimate the experienced delay at an intersection, the *Intersection Capacity Analysis* (ICA) has been developed by the Highway Capacity Manual (HCM) (TRB, 2016). This analysis takes traffic volumes as input and calculates the delays and capacity on each turn at the intersection. As a result, the delay is personalized for each route. Combining the ICA with a traffic assignment can provide more detailed solutions and better predictions of reality. However, it is not possible to directly implement the ICA in a traffic assignment. Beckman et al. (1956) have found that an optimal solution exists if the travel time is non-separable. In other words, the travel time on a road can only be affected by the circumstances on that road. However, the ICA uses aspects of different turns to determine the delay at intersections. To overcome this problem, the ICA is added as an external procedure to the traffic assignment. This has been realized as the *ICA assignment*, an iterative approach that executes a traffic assignment and ICA one after the other, such that an optimal solution is maintained. Moreover, the effects of congestion are included with the inclusion of a blocking back model. This model sets all traffic that exceeds capacities at turns back to links more upstream. This partly fills the gap between the omitted time aspect, since the ICA assignment is a static procedure.

Although the additional iterative intervention retains the unique property of the equilibrium, the solution is not stable. Small changes representing model errors result in large traffic shifts to other routes. Sawar et al. (2021) used the ICA assignment in their research to compare the output with real-life observations in Budapest. The travel times resulting from the ICA assignment differed significantly from the traffic survey data. Sawar et al. (2021) confirm the ambiguities in relating the ICA assignment output to the configuration of parameters.

The ability to explain the output based on the input parameters is crucial for establishing trust in traffic models. Without such an explanation, the reliability of the models is questionable. If a traffic model yields highly variable results with only slight input changes, it cannot be considered reliable or useful, even if some results might be according to expectations. These slight input changes represent small model errors that are likely to occur in each traffic model since it cannot make them fully accurate. In scientific research and modeling, it is essential that output changes can be deduced from its input. From a practical perspective, traffic models are used to anticipate traffic conditions and effectively plan interventions, such as traffic light timing adjustments, road expansions, and the implementation of intelligent transport systems. In scenario comparison, stable flows must be conserved. With an unstable output, the risk of implementing suboptimal or counterproductive measures increases, potentially resulting in congestion, accidents, and financial losses. Therefore, research must be done on the causes of instability in the ICA assignment and traffic models in general.

Previous research has not yet explored the stability of the ICA assignment. However, the ICA assignment model tends to be unstable in many circumstances. Since the ICA assignment is a relatively new development, its potential benefits and drawbacks are not yet understood. And, although the ICA assignment provides detailed delay calculations which lead to improved prediction of real-life situations, the unstable output cannot guarantee its value. Consequently, this thesis is set up to research the instability of the ICA assignment.

1.2 Research question

The main research question of this thesis is:

"How can the current instability appearing in the Intersection Capacity Analysis combined with a user equilibrium traffic assignment be alleviated?"

The main research question covers the problem of instability as well as possible interventions to the ICA assignment model. To facilitate the process of answering the research question, sub-questions are developed. These break down the process into steps that collectively address the main research question. The sub-questions are structured as follows:

1. What is the current state of instability of the ICA assignment?
    a. What is the convergence behavior when it is unstable?
2. Which input parameters impact the stability of the ICA assignment?
    a. What is the impact of the traffic assignment inside the ICA assignment?
    b. What is the impact of the blocking back model parameters?
3. What is the impact of various configurations of ICA intersections on stability?
4. Can parameter settings be adjusted such that the stability of the ICA assignment is improved?
    a. If yes, why do these parameters cause the ICA assignment to be more stable?

1.3 Thesis structure

The remainder of the thesis after this introduction is organized as follows. In Section 2, a theoretical literature review is conducted. This consists of all mathematical formulations used in this research together with a thorough explanation of the ICA assignment and its components. In Section 3, the methodology is formulated which describes the methods used to answer the research questions. It explains the contents of an elementary and real-life network, which will be used to execute experiments to parameter settings. Also, the stability assessment framework is defined which is used to make the stability measurable. Section 4 presents the results of all analyses that have been described in section 3. This will offer answers for the research sub-questions 1, 2, and 3. Subsequently, the outcome of each analysis is discussed, providing the answer to sub-question 4. Finally, Section 5 ends with a conclusion and recommendations for further research.

2 Theoretical framework

This section contains the theoretical framework of used methods. First, the theory of graph modeling is explained which transfers actual traffic networks into useful and feasible objects. The remainder is dedicated to a thorough explanation of the ICA assignment, detailing the mathematical principles underlying each component. The components of the ICA assignment are no unexplored territory. In the scientific literature, research has been done on traffic assignment applications. Three

types of traffic assignments will be used and compared in this study. For each, the algorithm is described and their mutual differences are highlighted. The ICA is presented with a step-by-step procedure, derived from the HCM 6th edition (TRB, 2016).

2.1 Network representation

In transport modeling, a traffic network is simplified to make it suitable for computational activities. This is done by developing a graphical representation of the network. A graph representation considers the network as a graph

$$\mathcal{G} = (\mathcal{N}, \mathcal{L}) \quad 1$$

Where $\mathcal{N}$ are the intersections represented as nodes and $\mathcal{L}$ the paths represented as links. Figures 1 and 2 illustrate the transformation of an arbitrary traffic network into a graph network.

Figure 1: Satellite view of an arbitrary traffic network (Google, 2024)

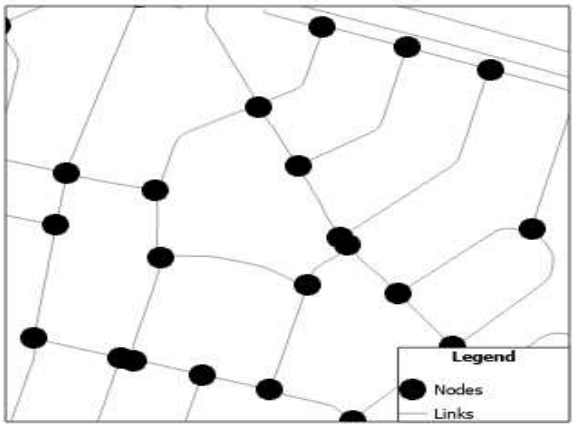

Figure 2: Own elaboration of graph representation of traffic network in Figure 1

Furthermore, additional notations within the graph network used in transport modeling need more attention. First of all, $\mathcal{T}$ are the turns that occur at a node and connect two links. Together with the nodes $\mathcal{N}$ and links $\mathcal{L}$, the turns $\mathcal{T}$ make up for the physical part of the graph network. Second, the locations of trip origins and destinations are captured in two separate sources. These are the origins $\mathcal{O}$ and destinations $\mathcal{D}$, respectively. Ideally, the origins and destinations should be linked to their exact graphical locations. Since this requires too much time to realize, the origins and destinations are connected to zones $\mathcal{Z}$ that covers an area of links and nodes. These zones are similar to neighborhoods, although they might deviate from the real boundaries. All trips leave and enter the zone from the center. The center is connected to the closest node, ensuring all traffic can reach it. When a vehicle travels from an origin to a destination, this can be described as a series of links and turns. Such a series is called a route, where its starting point must be linked to the set of origins and its endpoint to the set of destinations. Together, all routes form the set of routes $\mathcal{R}$. A full overview of all notations is given in Table 1.

Table 1: Notations in graph modeling

$\mathcal{N}$	Set of nodes in the graph network
$\mathcal{L}$	Set of links in the graph network
$\mathcal{T}$	Set of turns in the graph network
$\mathcal{O}$	Set of origins in the graph network
$\mathcal{D}$	Set of destinations in the graph network
$\mathcal{Z}$	Set of zones in the graph network
$\mathcal{R}$	Set of routes in the graph network

In the graph network $\mathcal{G}$, each link is subjected to a traffic demand q_{dem}, expressed in vehicles per hour. This is the traffic volume that wants to travel the link of concern. Furthermore, each link has its own cost to travel. This cost is derived from multiple factors captured in a *volume delay function* (VDF). A VDF is a function that describes the relationship between traffic demand and travel cost. Fixed parameters in the VDF describe the other factors influencing the travel cost. The structure of a VDF has many variations but the majority is based on the Bureau of Public Roads (BPR) function (1964). This function is shown in Equation 2:

$$t_{cur}^{l} = t_0^l * (1 + a^l * \left(\frac{q_{dem}^l}{q_{max}^l * c^l}\right)^{b^l} \quad 2$$

For a particular link $l \in \mathcal{L}$, a^l, b^l and c^l are the VDF coefficients, t_0^l the travel time in an unloaded graph network (at free-flow speed), q_{max}^l the capacity of the road section, q_{dem}^l the traffic demand and t_{cur}^l the travel time in a loaded graph network. Each link has a VDF with parameters adjusted to its characteristics. Turns impedances are also calculated with a VDF, with parameters controlled by the ICA. This will be further explained in the next section.

In the BPR formula, the travel cost is solely determined by the travel time. However, decision-making in route choice involves more factors than travel time alone. Consequently, a generalized cost value is formulated as a weighted sum of factors influencing the selection of routes. This generalized cost is known as "impedance" in the context of transportation and network analysis. Each traffic assignment determines the shortest paths based on the impedances. In this study, it is assumed that the impedance is a linear combination of travel time and travel distance. Then, the impedance of a link $l \in L$ is calculated as

$$t_{imp}^{l} = \beta_1 * t_{cur}^{l} + \beta_2 * d^l \quad 3$$

Here d^l is the length and t_{imp}^l the calculated impedance of link $l \in \mathcal{L}$. Furthermore, each term can be adapted with coefficients β_1, β_2 to precisely determine a generalized impedance that all travelers perceive equally. Since the distance term in the impedance calculation remains constant for each link, it is not included in the equations presented in the subsequent sections of this chapter. As a result, the impedance depends solely on the travel time, which relies on the traffic volume. Therefore, there is written $t_{imp}^l(q_{dem}^l)$ as impedance function for each link $l \in \mathcal{L}$.

2.2 The ICA assignment

The procedure of the ICA assignment is described in the manual for PTV Visum published by the PTV Group (2023). In Figure 3, the path from the start to the result of the ICA assignment is displayed as a flow chart. Initially, the VDFs for each link and turn are adjusted to their default settings. Then, there are three main steps. First, the subordinate assignment is performed where an equilibrium is reached in the network. This will generate a set of impedances based on the calculated demand for each link and turn. Second, a blocking back model is applied to smoothly divide volumes over the network (since the equilibrium does not consider link or turn capacities). This output contains adjusted traffic volumes, queue lengths, and wait times. Third, the intersection capacity analysis is performed according to the guidelines of the HCM (TRB, 2016), which delivers capacities and new turn impedances at the intersections where it is activated. Consecutively, the result of the ICA is used to recalibrate the VDFs of turns. The digression of new parameters for the turn VDFs relies on three sampling points. The first sampling point is the smoothed turn volume and the respective impedance computed with the ICA. The other two sample points are determined with slightly different smoothed turn volumes and their respective delays calculated by the ICA. A convergence check is performed after each iteration to control the results. If the results satisfy the convergence criteria or the maximum number of iterations is reached,

the procedure terminates and the current traffic assignment result is forwarded. In case of unsatisfied conditions, the VDFs for links and turns are updated to assimilate the blocking back results in the new iteration.

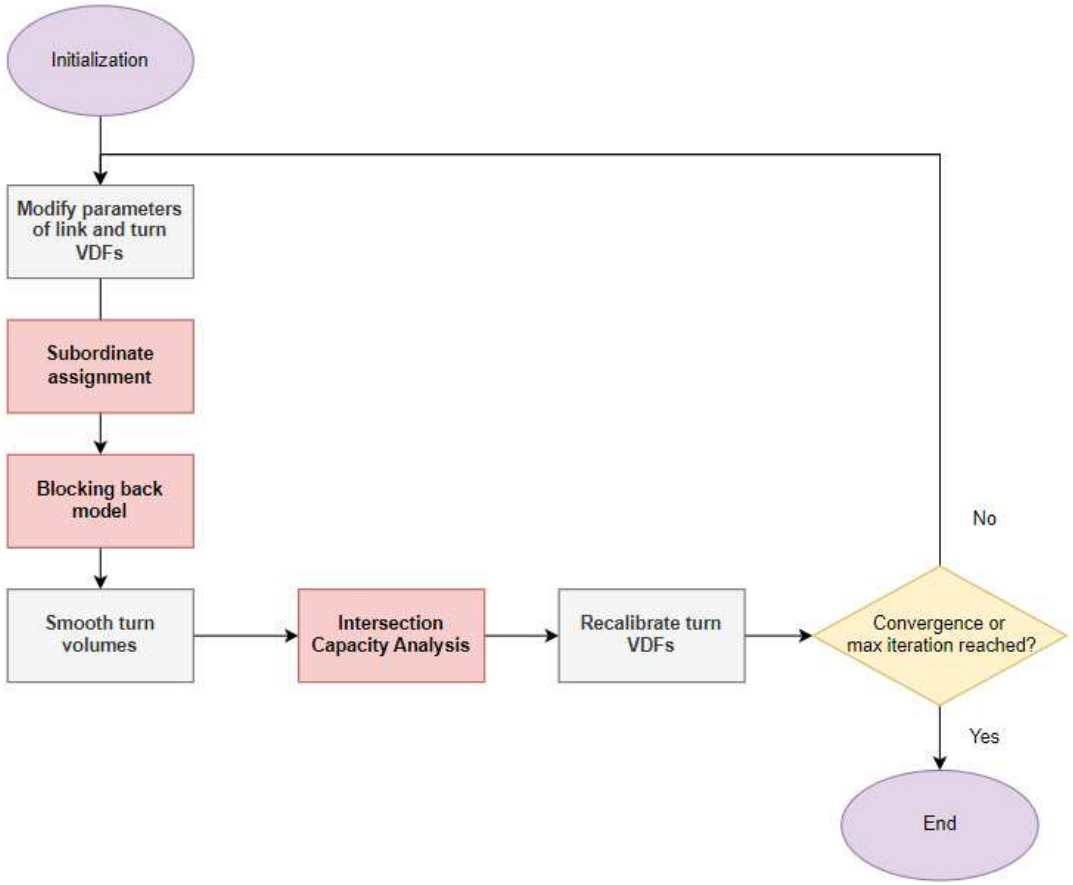

Figure 3: Systematic representation of the ICA assignment (own elaboration based on the procedure described in (PTV Group, 2023))

Within the procedure of the ICA assignment, most steps need more explanation to make the entirety clear. Therefore, the next sections will elaborate on the important steps in the ICA assignment.

2.2.1 Subordinate assignment

The subordinate or embedded assignment within the ICA assignment is the traffic assignment execution. An example of a traffic assignment result is the shortest route search. When demand for each OD pair is assigned to its shortest route, the traffic assignment is solved as an *All-Or-Nothing* (AON) assignment. This solution is not optimal, because the shortest paths are determined for an empty network. After an AON solution, the shortest paths are prone to change because new traffic volumes increase the travel time. Therefore, Beckman et al. (1956) stated the traffic assignment problem as an optimization problem, that required multiple steps to reach the optimal solution.

To find the optimal solution, a traffic situation must be solved as an *equilibrium* assignment, presenting a balanced traffic situation system in a network. An equilibrium assignment approaches the optimal solution iteratively, which makes it more time-consuming than an AON assignment. In each iteration, the solution gets closer to the optimal solution. When a solution gets sufficiently close to the optimal solution, the assignment will stop iterating and return the current solution. An equilibrium assignment

that aims to optimize the travel times for each traveler is a *user equilibrium* (UE) traffic assignment. The UE traffic assignment is universally accepted as the best practice for static traffic models and solves the optimization problem according to the first principle of Wardrop. The first principle of Wardrop states that no driver can reduce their travel costs by switching to another route (Wardrop, 1952). Furthermore, the UE performs under the assumption that all drivers have full information of all existing routes and will always take the ideal route to their destination (selfishness). The modeled route choice is *deterministic* when the perceived waiting time is equal to the actual waiting time. In this case, all travelers agree on the shortest routes and travel times in the network.

Within this thesis, the type of traffic assignments is limited to UE optimization. According to the optimization problem of Beckmann (1956), the UE is found by minimizing an objective function. This objective function sums all areas below the cost functions. Because the travel impedance is based on t_{cur}, it is a strictly increasing graph itself and can be used as a cost function in the objective function. Then, the objective can be written as shown in equation 4.

$$\sum_{l}^{\mathcal{L}} \int_{0}^{q_{dem}^{l}} t_{imp}^{l}(q_{dem}^{l}) dq_{dem} + \sum_{t}^{\mathcal{T}} \int_{0}^{q_{dem}^{t}} t_{imp}^{t}(q_{dem}^{t}) dq_{dem} \quad 4$$

Where, t_{imp} is the travel impedance in a loaded network and q_{dem} the travel demand. The objective function is the sum of all areas under the impedance VDFs of links and turns. In other words, by minimizing the total area under the VDF of the travel impedances for both links and turns, a user equilibrium is reached. When solving the minimization problem, the objective function is subjected to four constraints that set boundaries with regard to the minimization in the graph network. In Equation 5, 6, 7, and 8, the mathematical formulation of the constraints is given.

$$\sum_{r}^{\mathcal{R}} q_{ijr} = q_{ij}, \forall ij \in \mathcal{O}, \mathcal{D} \quad 5$$

$$q_{ijr} \geq 0, \forall ijr \in \mathcal{O}, \mathcal{D}, \mathcal{R} \quad 6$$

$$\sum_{r}^{\mathcal{R}} \sum_{j}^{\mathcal{D}} \sum_{i}^{\mathcal{O}} x_{ijr}^{t,l} q_{ijr} = q_{dem}^{t,l}, \forall l \in \mathcal{L}, \forall t \in \mathcal{T} \quad 7$$

$$\sum_{i}^{\mathcal{O}} q_{iz} - \sum_{j}^{\mathcal{D}} q_{zj} = \mathcal{D}_z - \mathcal{O}_z, \forall z \in \mathcal{Z} \quad 8$$

Where,

q_{ij}: the traffic volume between origin i and destination j
q_{ijr}: the traffic volume at route r between origin i and destination j
$x_{ijr}^{t,l}$: a binary variable which returns 1 if a link l or turn t is traveled by route r between origin i and destination j and 0 otherwise
$q_{dem}^{t,l}$: the traffic demand at link l or turn t

Constraint 3 states that for each origin and destination pair the sum of route volumes must be equal to the total volume. Constraint 4 ensures the non-negativity of traffic volume for each route that exists between each origin and destination pair. Constraint 5 extends constraint 3 to hold for all links and turns

as well. The sum of route volumes on each link or turn must be equal to the demand on that link or turn. At last, constraint 6 secures the conservation of traffic volume between a pair of zones, such that it matches the demand in the origin-destination matrix.

User equilibrium assignments are mainly classified into three categories: link-based, path-based, and bush-based. Link-based equilibrium assignments only consider the traffic demand and travel costs on links. Path-based assignments keep track of the route flows as well on top of the link flows. The main idea of a path-based algorithm is to find the solution by moving the flow of costlier paths to cheaper paths (Dafermos & Sparrow, 1969) (Jayakrishnan et al., 1994). Bush-based algorithms create sub-graphs for each origin that are connected to all destinations. For each sub-graph, the (local) equilibrium is found. When for each subgraph no better alternatives for drivers exist, the global minimum is found.

Throughout the years, many different algorithms have been developed to solve the traffic assignment problem which can serve as subordinate assignments in the ICA assignment. In the very beginning, the developed algorithms were link-based (Perederieieva et al., 2013). Because these algorithm types fail to provide higher precise solutions, path-based algorithms were proposed. Path-based algorithms need more computer memory storage than link-based algorithms since all paths must be stored as well. Although, it results in a much faster solution to the optimization problem (Dial, 2006). Later, bush-based algorithms were developed to achieve the same accuracy as path-based algorithms for even less computation time. The first bush-based assignment was developed by Bar-Gera (2002) and granted an equivalent computation speed with less memory space compared to the path-based algorithms.

In this study, there are three types of subordinate assignments considered: (1) a classical balancing equilibrium assignment (BEA) derived from the implementation in the manual of Visum (PTV Group, 2023); (2) the Bi-Conjugate Franke Wolfe (BFW) equilibrium assignment which is a comprehension of the original Frank-Wolfe (FW) equilibrium assignment (Mitradjieva & Lindberg, 2013) and; (3) the Local User Cost Equilibrium (LUCE) assignment, which is recently developed by Gentile (2014). The three assignments provide the costs for all links in the graph network but differ in a few perspectives. At first, the type of algorithm is different. The BEA has a similar operation as the algorithm described by Jayakrishnan et al. (1994) as it uses a balancing step where flow at non-shortest paths is set to shorter paths. Therefore, it is classified as path-based. The BFW is an extension of the FW algorithm, making it a link-based algorithm. LUCE is classified as a bush-based algorithm since it considers bushes in which all origins are connected to a single destination.

A second criterion that distinguishes the three traffic assignments is the level of proportionality in route distribution. Proportionality refers to the degree to which vehicles are divided in case two routes are equally attractive. When an algorithm always assigns vehicles to the same route even though their impedance is identical, proportionality is not achieved. (Xie & Nie, 2019). It has been proved that the condition of proportionality contributes to the uniqueness and stability of route flows, although its effect on link flow stability is not proved (Boyce et al., 2010) (Bar-Gera, 2010).

The final property of the traffic assignments is the relative gap which relates to the speed of convergence. The relative gap indicates the difference between a traffic assignment result and the situation when all vehicles are on their shortest path corresponding to their OD-relation (Patil et al., 2021). A common definition of the relative gap at a certain iteration k is given in Equation 9.

$$RG(k) = -\frac{gap(k)}{|BLB|} \tag{9}$$

$$gap(k) = AON(k) - CS(k) \leq 0 \tag{10}$$

$$BLB = \max_{k}(AON(k)) \tag{11}$$

Where the gap is defined by the distance away from the current solution $CS(k)$ to the AON solution (shortest paths) ($AON(k)$). BLB is the shortest path solution that is closest to the optimal solution (Boyce, Ralevic-Dekic, & Bar-Gera, 2004). These computations are shown in Equations 10 and 11, respectively.

A smaller gap leads to more accurate solutions but also more computational effort. Irrespective of the gap, the classical equilibrium assignment is the fastest of the three. With a relative gap of 1e-4, the BFW assignment outperforms the LUCE algorithm while a smaller relative gap of 1e-5 shows the opposite (PTV Group, 2023). In Table 2, the characteristics of the considered subordinate assignments are summarized.

Table 2: Characteristics of subordinate assignments (own elaboration based on (PTV Group, 2023))

	Type	**Proportionality of demand**	**Computation speed (Gap 10^{-3})**	**Computation speed (Gap 10^{-4})**	**Computation speed (Gap 10^{-5})**
BEA	Path-based	Not achieved	++	+	+
BFW	Link-based	Fully achieved	0	0	-
LUCE	Bush-based	Partially achieved	-	0	0

In the next three subsections, each of the three equilibrium assignments is thoroughly explained and their step-wise algorithm is presented.

2.2.1.1 Classical Balancing Equilibrium Assignment (BEA)

The classical user equilibrium assignment solves the optimization problem with an iterative procedure. This procedure is elaborated in this section based on the implementation as shown in the manual of Visum (PTV Group, 2023). After an initial suboptimal traffic assignment is carried out, vehicles at costly routes will be shifted to routes with lower cost, such that routes connecting the same OD-pairs have the same impedance. This balancing step is done for all OD pairs. This is how the procedure moves toward the minimum of the objective function. After the balancing step, a shortest path search is performed for every OD pair to identify possible new routes that result in a lower impedance. If this is the case, a new balancing of traffic volumes is performed. The stepwise scheme is shown below for a given iteration k:

- **Step 1**: (Initialization). Load the network by executing an all-or-nothing (AON) assignment to create a starting point $q_{dem}^{0,t,l}$ and $t_{imp}^{0,t,l}(q_{dem}^{0,t,l})$ for each link $l \in \mathcal{L}$ and turn $t \in \mathcal{T}$. Furthermore, it calculates the volumes q_{ij}^{0} and q_{ijr}^{0} at routes $r \in \mathcal{R}$ between origin $i \in \mathcal{O}$ and destination $j \in \mathcal{D}$.
- **Step 2:** (Volume Balancing). Balance the traffic volumes q_{ijr}^{0} by shifting volumes of routes with high impedance to routes with low impedance. This gives new values for $q_{dem}^{k,t,l}$, $t_{imp}^{k,t,l}(q_{dem}^{k,t,l})$, q_{ijr}^{k} and q_{ij}^{k}.
- **Step 3:** (New Routes). Calculate new routes with updated impedance because of the balancing in **step 2**.
- **Step 4:** (Convergence). The procedure converges if there are no new routes that give a lower impedance than any existing route. Otherwise, there is returned to **step 2** and the iteration counter is incremented by one**.**

When the procedure terminates, the final values for the demand $q_{dem}^{t,l}$ and travel impedance $t_{imp}^{t,l}(q_{dem}^{t,l}), \forall l \in \mathcal{L}, \forall t \in \mathcal{T}$ are stored and used in the next step of the ICA assignment.

2.2.1.2 *Equilibrium Assignment Bi-Conjugate Frank Wolfe (BFW)*

The BFW equilibrium assignment takes a different approach to finding the minimum of the objective. Mitradjieva & Lindberg (2013) have developed the BFW algorithm and wrote a scientific paper in which the improved performance of their new asset is confirmed. In the context of computational effort, the BFW scores higher compared to the traditional Franke Wolfe (FW) and the Conjugate Franke Wolfe (CFW), while achieving the same accuracy of the solution.

Initially, a starting situation is needed such as an AON assignment as input for the algorithm. Then, the curve of the impedance function t_{imp} is approximated with the first Taylor expansion. A search direction is determined by minimizing the first Taylor expansion over q_{dem}, and subtract the current value of q_{dem}. Finally, a step size is calculated by minimizing the cost function as a linear combination of the current demand and search direction. A new point is calculated by moving towards the search direction with the found step size. When there is no new search direction, the minimum is achieved and the algorithm terminates. The stepwise procedure is shown below for a given iteration number k:

- **Step 1: (**Initialization). Load the network by executing an all-or-nothing (AON) assignment or incremental assignment to create a starting point $t_{imp}^{0,t,l}(q_{dem}^{0,t,l})$ for each link $l \in \mathcal{L}$ and turn $t \in \mathcal{T}$.
- **Step 2:** (Approximate cost functions). The first Taylor expansion describes the cost function by

$$t_{imp}^{k,t,l}(q_{dem}) = t_{imp}(q_{dem}^{k,t,l}) + \nabla t_{imp}(q_{dem}^{k,t,l})^T (q_{dem} - q_{dem}^{k,t,l}) \quad 12$$

- **Step 3**: (Search direction) A search direction is determined by minimizing the first-order Taylor expansion. Since q_{dem} only appears in the second term, the point of sight becomes

$$y_k^{FW} = \min\left(\nabla t_{imp}(q_{dem}^{k,t,l})^T (q_{dem})\right) \quad 13$$

  Then, the search direction is

$$d_k^{FW} = y_k^{FW} - q_{dem}^{k,t,l} \quad 14$$

  The BFW differs from the FW in the way it determines the search direction. For the BFW, the search directions of two previous iterations are used to determine the new search direction. This gives the search direction

$$d_k^{BFW} = \beta_k^0 d_k^{FW} + \beta_k^1 (s_{k-1}^{BFW} - q_{dem}^{k,t,l}) + \beta_k^2 (s_{k-2}^{BFW} - q_{dem}^{k,t,l}) \quad 15$$

  Where s_{k-1}^{BFW} and s_{k-2}^{BFW} are the point of sight determined with BFW in the previous $k-1$ and $k-2$ iterations, respectively. The values for β_k^0, β_k^1 and β_k^2 are determined from previous iteration values and these derivations are shown in Appendix A.

- **Step 4:** (Line Search). Minimizing the objective function that moves into the new descent direction gives the step size

$$\gamma_k = argmin\left(t_{imp}(q_{dem}^{k,t,l} + \gamma_k d_k^{CFW})\right) \quad 16$$

- **Step 5**: (Update). Update the demand and cost functions

$$q_{dem}^{k+1,t,l} = q_{dem}^{k,t,l} + \gamma_k d_k^{BFW} \quad 17$$

$$t_{imp}^{k,t,l}\left(q_{dem}^{k,t,l}\right) = t_{imp}^{k+1,t,l}\left(q_{dem}^{k+1,t,l}\right) \quad 18$$

- **Step 6:** (Convergence). The procedure converges if there is no new search direction that gives a lower impedance than any existing route. Otherwise, there is returned to **step 2.**

When the procedure terminates, the final values for $q_{dem}^{t,l}$ and travel impedance $t_{imp}^{t,l}\left(q_{dem}^{t,l}\right), \forall l \in \mathcal{L}, \forall t \in \mathcal{T}$ are stored and used in the next step of the ICA assignment.

2.2.1.3 Linear User Cost Equilibrium Assignment (LUCE)

In contrast to the previous two algorithms, LUCE is a bush-based equilibrium assignment. It will solve multiple local equilibria for all bushes in the network. A bush is the set of all nodes and links that are used when connecting all destinations to one origin if there is any demand. Conversely, Gentile (2014), the founder of the LUCE algorithm, constructed bushes by linking all origins to each destination. Thus, there are as many bushes as destinations and for all a local user equilibrium is established. Similar to the BFW, it uses the linear approximation of the cost functions to find a descent direction. Additionally, the costs to get from a node to the destination and its derivative is calculated, for each node in the graph.

Before the computation of the search direction, the current bush is initialized and potentially improved by excluding inefficient links. Efficient links are categorized into three types of efficiencies:

1. Graph-efficient. For each node, links that get closer to the destination on the graph are included in the bush.
2. Bush-efficient. For each node, links that get closer to the destination of the bush in terms of *node minimum* costs are included in the bush.
3. Max-efficient. For each node, links that get closer to the destination of the bush in terms of *node maximum* costs are included in the bush.

Then, the local equilibrium cost for each node in the bush is determined, which is again used to determine the auxiliary flow of the search direction on links. Finally, an Armijo step is applied to determine the step size. The Armijo rule is a backtracking line search method that decreases the step size with a predefined factor until the objective function toward the search direction is feasible. When this is satisfied, the demand and cost functions are updated with the found step size towards the search direction. Once all bushes cannot be improved by any of the three efficiency steps, the algorithm will terminate. A stepwise explanation is given below for a given iteration k and destination d.

- **Step 1:** (Initialization). Determine starting point $q_{dem}^{k,ij}$ such that the cost function is $t_{imp}^{k,ij}\left(q_{dem}^{k,ij}\right), \forall ij \in \mathcal{L}, \mathcal{T}$ in the network, and $i, j \in \mathcal{N}$. Determine the derivative of $t_{imp}^{k,ij}(q_{dem}^{k,ij})$, $\nabla t_{imp}^{k,ij}(q_{dem}^{k,ij})$.
- **Step 2:** (Bush modification). Initialize and modify bushes with

$$B(d) = \left\{i, j \in \mathcal{N} : W_i^d > W_j^d\right\} \quad 19$$

$$B(d) = \left\{i, j \in \mathcal{N} : \widehat{W}_i^d > \widehat{W}_j^d\right\} \quad 20$$

$$B(d) = \left\{i, j \in \mathcal{N} : U_i^d > U_j^d\right\} \quad 21$$

Where Equations 19, 20, and 21 present the graph-efficiency, bush-efficiency, and max-efficiency respectively. W_i^d and W_j^d are the minimum costs to reach destination $d \in \mathcal{D}$ from

node $i, j \in \mathcal{N}$ on graph $\mathcal{G}$, respectively. $\widehat{W}_i^d$ and $\widehat{W}_j^d$ are the minimum costs to reach destination $d \in \mathcal{D}$ from node $i, j \in \mathcal{N}$ on bush $B(d)$, respectively. U_i^d and U_j^d are the maximum costs to reach destination $d \in \mathcal{D}$ from node $i, j \in \mathcal{N}$ on bush $B(d)$.

- **Step 3:** (Node costs). For each node $i \in \mathcal{N}$ connected to the bush formed by destination $d \in \mathcal{D}$, the node's average cost to reach the destination and its derivative is calculated by

$$C_i^d = \sum_{j \in FSB(i,d)} y_{ij}^d * \left(t_{imp}^{k,ij}(q_{dem}^{k,ij}) + C_j^d \right), \qquad \forall i \in B(d) \tag{22}$$

$$G_i^d = \sum_{j \in FSB(i,d)} \left(y_{ij}^d \right)^2 * \left(\nabla t_{imp}^{k,ij}(q_{dem}^{k,ij}) + G_j^d \right), \qquad \forall i \in B(d) \tag{23}$$

Here, C_i^d and C_j^d are the average costs to reach destination $d \in \mathcal{D}$ from node $i \in B(d)$, G_i^d and G_j^d the derivatives of the average costs to reach destination $d \in \mathcal{D}$ from node $i \in B(d)$ and y_{ij}^d the flow proportion at link and turn $ij \in \mathcal{L}, \mathcal{T}$ towards destination $d \in \mathcal{D}$. The flow proportion at each link is calculated with

$$y_{ij}^d = \frac{q_{dem,d}^{k,ij}}{q_{dem,d}^{k,i}}, \qquad ij \in \mathcal{L}, \mathcal{T} \tag{24}$$

- **Step 4:** (Convergence). Convergence is reached when the stop criteria are met for the current destination. If so, there is moved to the next destination and returned to **step 1.** If not, the LUCE search direction is computed in the next step.
- **Step 5:** (LUCE search direction). First, the node cost functions V_i^d for node search directions e_i^d are determined. All e_i^d are equal to the demand if there is any and otherwise 0. Then, the arc search directions e_{ij}^d are determined by the results of V_i^d for all j that are in the forward star of i to d. The forward's star $FSB(i,d)$ contains the bush network of nodes and links that can be reached when traveling from node i to destination d.

$$V_i^d = \frac{e_i^d + \sum_{j \in J} \left(\left(\frac{t_{imp}^{k,ij}(q_{dem}^{k,ij}) + C_j^d}{\nabla t_{imp}^{k,ij}(q_{dem}^{k,ij}) + G_j^d} \right) e_i^d * y_{ij}^d \right)}{\sum_{j \in J} \frac{1}{\nabla t_{imp}^{k,ij}(q_{dem}^{k,ij}) + G_j^d}}, \qquad \forall i \in B(d) \tag{25}$$

$$e_{ij}^d = \frac{V_i^d}{\nabla t_{imp}^{k,ij}(q_{dem}^{k,ij}) - G_j^d} - \frac{t_{imp}^{k,ij}(q_{dem}^{k,ij}) + C_j^d}{\nabla t_{imp}^{k,ij}(q_{dem}^{k,ij}) + G_j^d} + e_i^d y_{ij}^d, \quad \forall i \in B(d), \forall j \in FSB(i,d) \tag{26}$$

The node search directions e_j^d are updated with the arc search directions e_{ij}^d.

$$e_j^d = e_j^d + e_{ij}^d, \qquad \forall i \in B(d), \forall j \in FSB(i,d) \tag{27}$$

- **Step 6:** (Armijo Step). The Armijo step is performed to determine the **step length.** The directional derivative is the sum of the dot product of the objective function moving to the search direction and the search direction itself. Then, the feasible region is reached for values of α such that the directional derivative is negative.

$$until \sum_{i,j \in \mathcal{N}} t_{imp}^{k,ij}\left(q_{dem}^{k,ij} + \alpha * \left(e_{ij}^{d} - q_{dem,d}^{k,ij}\right)\right) * \left(e_{ij}^{d} - q_{dem,d}^{k,ij}\right) < 0 \quad 28$$

$$do\ \alpha = \frac{1}{2}\alpha \quad 29$$

- **Step 7:** (Update). Update the demand and cost functions, proceed to the next iteration and destination and return to **Step 1.**

$$q_{dem}^{k+1,ij} = q_{dem}^{k,ij} + \alpha_k * \left(e_{ij}^{d} - q_{dem,d}^{k,ij}\right), \forall ij \in \mathcal{L}, \mathcal{T} \quad 30$$

$$t_{imp}^{k,ij}\left(q_{dem}^{k,ij}\right) = t_{imp}^{k+1}\left(q_{dem}^{k+1,ij}\right) \quad 31$$

When the procedure terminates, the final values for $q_{dem}^{t,ij}$, $t_{imp}^{t,ij}(q_{dem}^{t,ij})$, $\forall ij \in \mathcal{L}, \mathcal{T}$ are stored and used in the next step of the ICA assignment.

2.2.2 Blocking back model and smoothed turn volumes

Irrespective of the type of equilibrium assignment being used, the output provides the traffic demand q_{dem} and impedance t_{imp} for each link and turn in the network. The blocking back model is a pseudo-dynamic assignment that is used in static traffic models to incorporate the effects of congestion (PTV Group, 2023). Because static traffic models do not consider effects over time, queues and waiting times as a consequence of congestion cannot be captured. By modifying traffic volumes at locations where the demand exceeds the capacity, the effects of congestion are considered within the ICA assignment. The procedure of blocking back is shown with an example of three links and two nodes, where traffic flow is moving in the right direction. In Figure 4, the traffic moves at a free flow speed of 600 veh/h, and no queuing is observed. When a bottleneck occurs at the intersection such that only 400 veh/h can pass, a queue is formed on the links upstream of the bottleneck intersection depicted in red in Figure 5. As a result, the travel time will increase on the queued links and decrease on links downstream of the bottleneck.

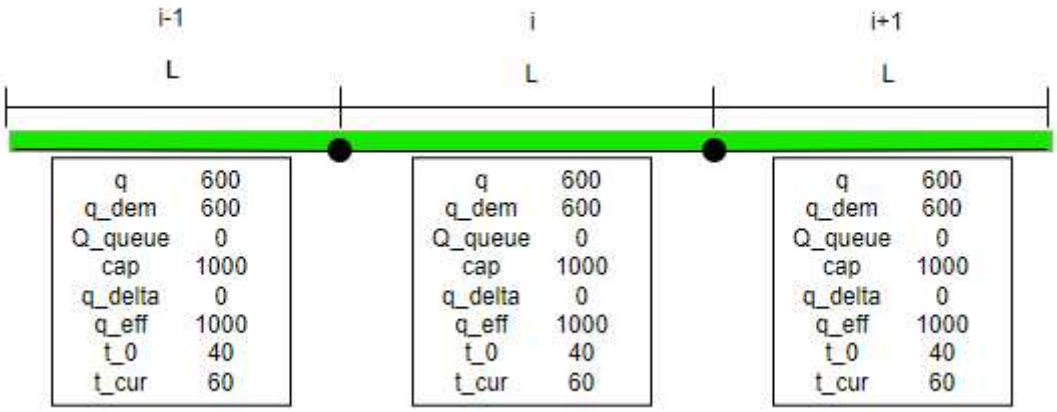

Figure 4: Freeflow state of traffic situation

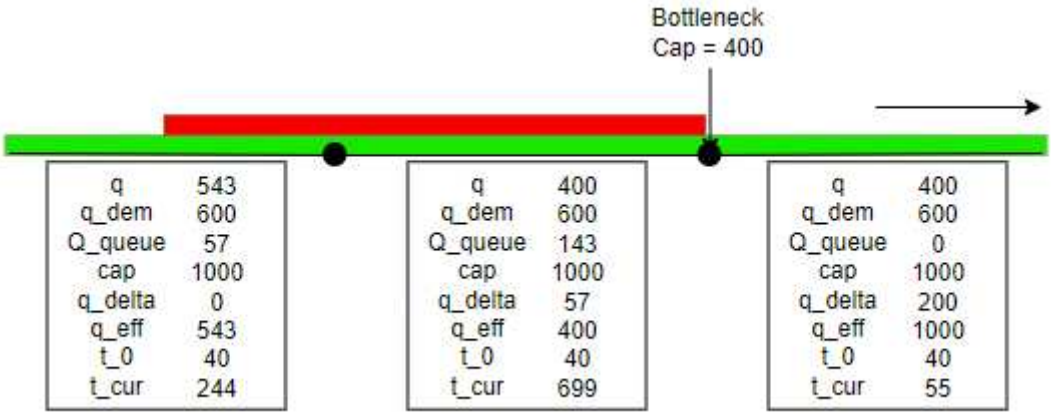

Figure 5: Congested state of traffic situation due to bottleneck

The variables of link i are determined as follows:

$$Q_{queue}^{i} = \min\left(q_{delta}^{i+1}, \frac{L^{i}}{x}\right) \quad 32$$

$$q_{delta}^{i} = q_{dem}^{i} - \left(q^{i} + Q_{queue}^{i}\right) \quad 33$$

$$q_{eff}^{i} = \begin{cases} cap^{i}, if\ Q_{queue}^{i} = 0 \\ q^{i}, if\ Q_{queue}^{i} > 0 \end{cases} \quad 34$$

$$t_{cur,BB} = \frac{\frac{I}{2}}{q_{eff}^{i}}\left(Q_{queue}^{i}\right) \quad 35$$

Where

Q_{queue}^{i}: the queue length at link i in meters
q_{delta}^{i}: is the traffic pressed upstream in veh/h
L^{i}: the length of link i in meters
x: the average car length in meters
q^{i}: the actual traffic at link i in veh/h
cap^{i}: the capacity of link i in veh/h
q_{eff}: the effective capacity of link i in veh/h
I: the assignment period in seconds
$t_{cur,BB}$: the travel time calculated by blocking back in seconds

The blocking back model calculates the variables above for all links in a fixed number of slices. The number of slices indicate the volume share of q_{dem} that is distributed over the network at a single time. As a result, one blocking back slice s considers a traffic demand of

$$q_{dem}^{s} = \frac{q_{dem}}{S} \quad 36$$

Where S is the total number of volume shares and q_{dem}^{s} the traffic demand at slice s. The result of the blocking model causes the actual demand $q^{l} \ \forall l \in \mathcal{L}$ to be equal to or lower than the traffic demand q_{dem} because of capacity constraints at nodes and potential links.

After the traffic variables are updated by blocking back, a smoothing step is performed for the turn volumes q^{t}. This step balances the turn volumes from the current and previous iteration if there are any. For the first iteration, the smoothed turn volume is equal to the turn volume of that iteration. The smoothed turn volume is described as

$$q_{smoothed} = q^{t,n-1} + f * (q^{t,n} - q^{t,n-1}) \quad 37$$

Where f is a smoothing factor, ranging between 0 and 1. The smoothed turn volumes serve as input for the ICA at nodes. This procedure is explained in the next section.

2.2.3 Intersection Capacity Analysis (ICA)

The nodes $\mathcal{N}$ in the network often contains much more detail than shown in the graphical representation of a traffic network. Therefore, the nodes are expanded with a nested representation, which is used for the ICA. An example of such a representation is shown in Figures 6 and 7, which is a typical busy signalized intersection.

Figure 6: Arbitrary intersection in real world (Google, 2024)

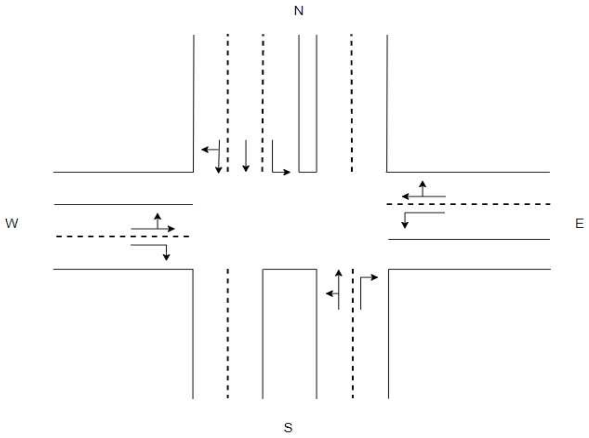

Figure 7: Own elaboration of graph representation of the intersection in Figure 6

As stated before, the ICA is used to determine the delay (impedance) and capacity of intersections. Intersection delay is a complex task because of the non-deterministic nature of arrival and departure processes. Traditional delay models use a VDF to describe the delay of intersections, but fall short of capturing the stochastic effects (Webster, 1958) (Akcelik, 1981) (Robertson, 1979). The ICA tries to include sufficient details such that these stochastic effects can be approximated as accurately as possible. At signalized intersections, the delay variation is enhanced by interruption of traffic flows due to traffic signals. Therefore, the ICA is particularly useful for intersections with signalization. As a result, the ICA is solely committed to signalized intersections in this research. The delays and capacity of unsignalized intersections will be determined with regular node VDFs.

Using the smoothed turn volumes, the delay and capacities of signalized intersections are computed. The ICA follows the steps of the HCM for signalized intersections. The HCM is the first appearance that was able to incorporate intersections in planning methodology (Transportation Research Board of the National Academies, 1985). Its standards and guidelines have widely been used in the field of transport modeling and traffic operations. Therefore, the manual has been updated through the years to maintain its dexterity. The methodology followed in HCM to determine delay and capacity at signalized intersections is a step-wise iterative program that eventually returns the performance of an intersection,

expressed in the Level Of Service (LOS). Furthermore, it calculates the capacity and delay $t_{cur,ICA}^{t}$ for each turn. An overview of the procedure is shown in Figure 8.

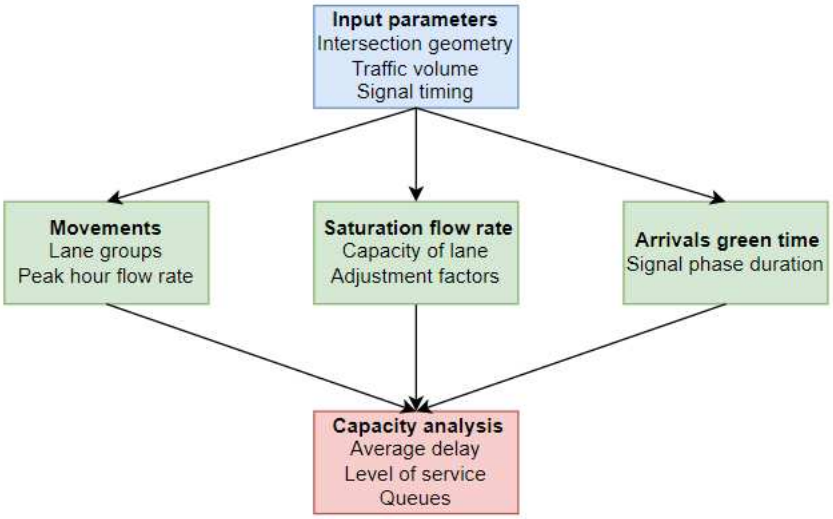

Figure 8: Flow chart of the intersection capacity analysis (own elaboration based on the methodology of the HCM 6th edition)

For the execution of the ICA, three types of input parameters are needed. The intersection geometry, traffic volume and the phasing of the traffic lights. In total, 9 steps are distinguished and their operation is described for a single example intersection. First, an overview of the notations used for the ICA is given in Table 3.

Table 3: Notations in the ICA procedure

PARAMETER	DESCRIPTION	UNIT
s_0	Base saturation flow rate	Vehicle/hour/lane
f_w	Adjustment factor for lane width	-
f_{LU}	Adjustment factor for lane utilization	-
f_{LT}	Adjustment factor for left-turn vehicle presence in a lane group	-
f_{RT}	Adjustment factor for right-turn vehicle presence in a lane group	-
R_p	Platoon ratio	-
g	Green time of lane group	Seconds
C	Cycle time of signalization	Seconds
c	Capacity of a lane group	Veh/h
N	Number of lanes	Lane
d_1	Uniform delay	Seconds/vehicle
d_2	Incremental delay	Seconds/vehicle
d_3	Initial queue delay	Seconds/vehicle

Step 1: Determine the movement groups and lane groups

Initially, all movement groups and lane groups at the intersection must be identified. Movement groups indicate each direction of movement and lane groups include the lanes that move into these directions. Thus, there may be more movement groups than lane groups in the case of *shared* lane groups.

Step 2: Determine the movement group flow rate

The smoothed turn volumes are connected to the movement groups. This ends up with the base volumes in each direction of the intersection.

Step 3: Determine the lane group flow rate

Instead of movement groups, the lane groups consist of all lanes that enter the intersection. In case of shared lanes, multiple movement groups are included in the lane group. For each lane, the base volume is determined. Furthermore, the proportion of vehicles turning left and right is derived.

Step 4: Determine the adjusted saturation flow rate

Based on the lane groups, the adjusted saturation flow rate is computed. It consists of the base saturation flow rate corrected by a set of adjustment factors that influence the traffic flow. The base saturation flow rate is the flow that can be handled by a lane group if the traffic light is green fulltime. The adjusted saturation flow rate is then calculated as

$$s = s_0 N f_w f_{LU} f_{LT} f_{RT} \tag{38}$$

Where all factors take a value between 0 and 1, in the actual derivation for the adjusted saturation, a more detailed calculation is used with more factors included. Because of the scope limitation in this thesis, the majority of the adjustment factors will be 1 and excluded in equation 38. An elaboration of the adjustment factors that fall within the scope of this work is given in Appendix B.

Step 5: Determine the proportion arriving during green

The delay experienced by a lane group is strongly dependent on the timing of vehicle arrivals. The proportion of vehicles arriving during green time can be calculated with the platoon ratio and green time ratio as given below:

$$P = R_p \left(\frac{g}{C}\right) \tag{39}$$

However, it is assumed that all vehicles will uniformly arrive at the intersection. Therefore, the platoon ratio is always 1 and the proportion of vehicles arriving at green time is equal to the green time ratio of that lane.

Step 6: Determine capacity and volume-to-capacity ratio

With the calculations in previous steps, the capacity of the lane groups can be resolved. The capacity in vehicles/hours/lane is calculated as

$$c = N * s * \frac{g}{C} \tag{40}$$

Volume-to-capacity ratio is determined by

$$X = \frac{v}{c} \tag{41}$$

Where v is the demand flow rate (veh/h) retrieved from the lane group flow rate in step 3.

It is important to determine the critical intersection volume-to-capacity ratio. This can be measured by adding the critical phases at an intersection. The critical intersection volume-to-capacity is computed as

$$X_c = \left(\frac{C}{C-L}\right)\sum_{i \in ci} y_{c,i} \quad 42$$

Where

$$y_{c.i} = \frac{v_i}{N * s_i} \quad 43$$

$$L = \sum_{i \in ci} l_{t,i} \quad 44$$

Where ci is the set of critical phases and $l_{t,i}$ the lost time at phase i.

Step 7: Determine the delay

The delay for each lane group is the sum of three types of delay: uniform delay, incremental delay, and initial queue delay, all expressed in seconds/vehicle. Uniform delay shows up with arrivals as they occur in an average cycle throughout the analysis period. Incremental delay is an extra delay to account for random, cycle-by-cycle fluctuations in demand that exceed capacity and extra delay to account for sustained oversaturation during the analysis period. In the uniform and incremental delay estimation, no initial queue is assumed. To account for this, the delay caused by the initial queue is added. Transferring the definitions of delay to an equation leads into

$$d = d_1 PF + d_2 + d_3 \quad 45$$

Where d is the total delay of the lane group, d_1 the uniform delay, d_2 the incremental delay, d_3 the initial queue delay and PF a progression factor. The factor reflects the signal coordination at an intersection that has an effect on adjacent intersections. As such, with good signal coordination, the average delay decreases (Hillier & Rothery, 1967). The calculation for PF, d_1, d_2 and d_3 are further worked out in Appendix C. The delay for the entire approach is calculated based on volumes from each lane group and the corresponding delays. Then

$$d_A = \frac{\sum d_i * v_i}{\sum v_i} \quad 46$$

The delay for the entire intersection is determined likewise but uses the volumes of the approaches and the corresponding calculated delays from equation 46.

$$d_I = \frac{\sum d_A * v_A}{\sum v_A} \quad 47$$

Step 8: Determine the Level Of Service

With the calculated delays, a score can be given to each of the approaches. This is done by the Level Of Service (LOS). LOS is an indication of the general acceptability of the delay levels at the intersection and ranges from values between A and F. The value is given according to the definition in Table 4.

Table 4: Level of service notations

LOS	Mean delay (seconds/vehicle)
A	0-10
B	10-20
C	20-35
D	35-55
E	55-80
F	80+

Step 9: Determine the Queue Length

The final step determines the queue storage ratio which indicates the available queue space. First, the mean queue length is determined for each lane group:

$$Q = Q_1 + Q_2 \tag{48}$$

Where Q_1 is the length of queued vehicles that occurs during uniform arrivals and Q_2 the queue length that emerges during random arrivals. An elaboration of the derivation of the queue lengths is found in Appendix D.

2.2.4 Turn VDF adjustment

With the results of the ICA, a different delay is found than the delay calculated with the current VDF for turns. Therefore, the parameters for each turn VDF are recalibrated. In this way, the new turn VDFs return the calculated delay by ICA with the given smoothed turn volume. In Figure 9, a visualization is shown of the recalibration procedure. The new parameters are found by interpolating a line through three points. These points are delays calculated with ICA for three different instances of turn-smoothed volumes, depicted as $t_{cur,ICA}(q_{smoothed}), t_{cur,x}(q_x)$ and $t_{cur,y}(q_y)$. Because the structure of the VDF is known, three points are enough to retrieve the values of the new parameters A, B and t_0. As a result, the new turn VDF becomes

$$t_{curICA} = t_{0,new} + A_{new} * \left(\frac{q_{smoothed}}{cap_{ICA}}\right)^{B_{new}} \tag{49}$$

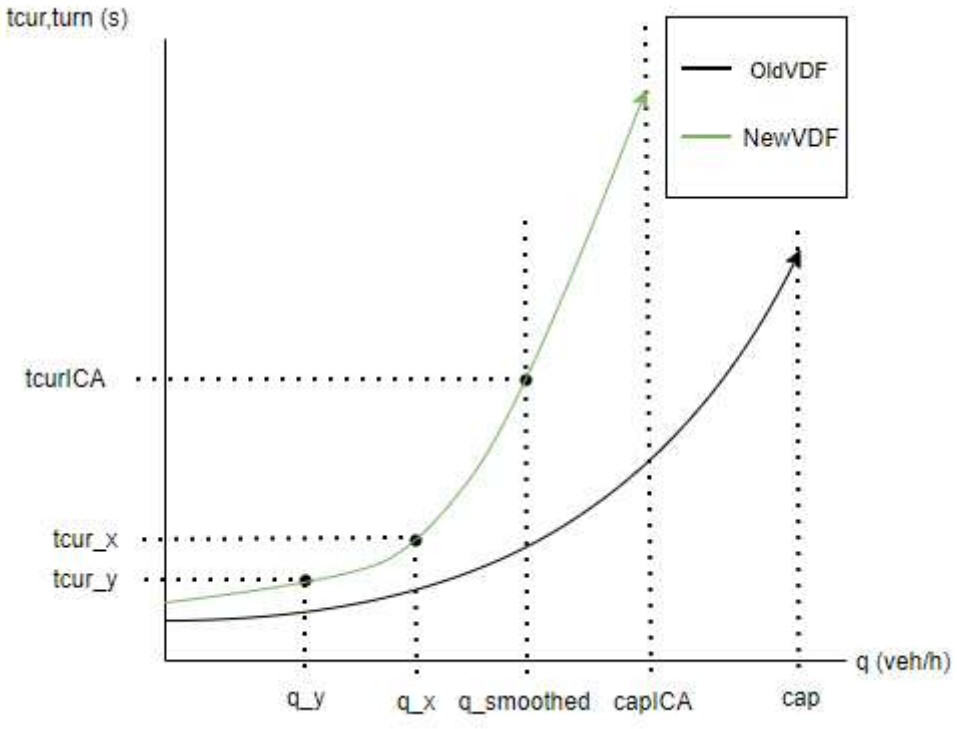

Figure 9: Turn VDF recalibration

2.2.5 Convergence criteria

At the end of each iteration, the algorithm checks if convergence is reached conceding that the maximum number of iterations has not been reached yet. The convergence criteria consist of six conditions that must all be fulfilled in order to successfully terminate the assignment. The first three conditions are composed according to the Geoffrey E. Havers (GEH) statistic. This statistic is a common application

in the field of traffic engineering to compare traffic volumes of models and real-world results with each other. The GEH value is computed as shown in equation 50.

$$GEH = \sqrt{\frac{2(M-C)^2}{M+C}} \qquad 50$$

Where M are the modeled results and C the counts or observed results. In the ICA assignment, the input variables for the GEH statistic consist of the values being compared in the condition. The fourth and fifth conditions are determined by relative deviation. The final condition is determined by an average absolute difference. In table 5, the six conditions are then given as follows.

Table 5: Conditions for convergence

Number	Condition
1	$\sqrt{\frac{2\left(q_{i,link} - q_{i-1,link}\right)^2}{q_{i,link} + q_{i-1,link}}}$
2	$\sqrt{\frac{2\left(q_{i,turn} - q_{i-1,turn}\right)^2}{q_{i,turn} + q_{i-1,turn}}}$
3	$\sqrt{\frac{2\left(q_{i,turn} - q_{i,smoothed}\right)^2}{q_{i,turn} + q_{i,smoothed}}}$
4	$\frac{\left\lvert t_{cur,link} - t_{cur,BB}\right\rvert}{t_{cur,link}}$
5	$\frac{\left\lvert t_{cur,turn} - t_{cur,ICA}\right\rvert}{t_{cur,turn}}$
6	$\frac{\left\lvert Q_{queue,i} - Q_{queue,i-1}\right\rvert}{\sum_{all\ congested\ links} 1}$

The first condition looks at the values of link traffic volumes of the current and previous iteration. The same applies for the second condition but on turn level. Condition 3 compares the turn volumes with the smoothed turn volumes. The latter two conditions look at the differences in delay. Condition 4 is the difference between the delay calculated from link VDF functions and the additional delay by blocking back. Condition 5 checks the heterogeneity of the delay from the turn VDF and the delay calculated with ICA. At last, condition 6 sets a boundary to the average difference of queues at links. Any condition is fulfilled when its value reaches a predefined threshold. Because a condition is applied to a single link or turn only, it must be fulfilled for a certain percentage of all links or turns. This is defined as the condition shares. When one condition fails to meet the share-defined percentage, the ICA assignment goes back to the previous step and increments the iteration counter. Besides, the link- and turn VDFs are modified as explained in the next section.

2.2.6 Link- and turn VDF modification

If the ICA assignment did not converge, the results of the blocking back model are processed in the existing VDFs for both links and turns. The blocking back model calculated spillback caused by capacity exceedance. Some turns cannot be reached because of the capacity limitation which should be incorporated in the turn VDFs. Figure 10 shows what alteration is done to the VDFs of turns that are located at intersections that encounter less traffic because of the blocking back model. The traffic that cannot enter the turns is q_{delta}, the traffic volume that is shifted upstream. As a result, the VDF is shifted to the left with q_{delta}.

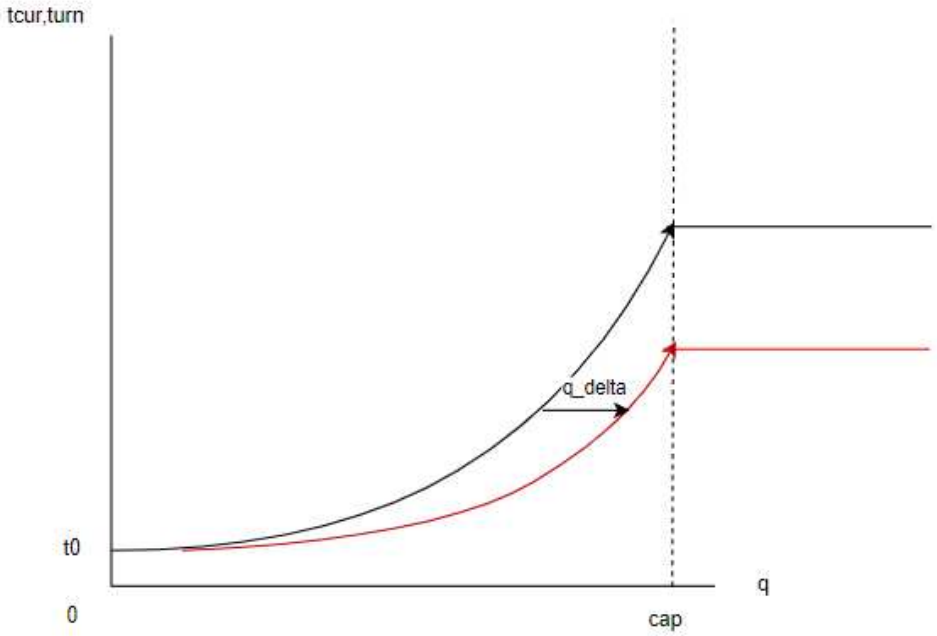

Figure 10: Turn VDF modification

With the shift of q_{delta}, the new turn VDF can be rewritten as shown in equation 51.

$$t_{cur,turn} = t_{0,new} + A_{new} * \left(\frac{q_{smoothed} - q_{delta}}{cap_{ICA}}\right)^{B_{new}} \quad 51$$

For links, the shift of the VDF applies as well. Traffic cannot reach some links because of bottlenecks further upstream such that the traffic demand is not met. On top of that, links can experience queues caused by bottlenecks downstream. In Figure 11, the result of both modifications on a single link VDF is shown.

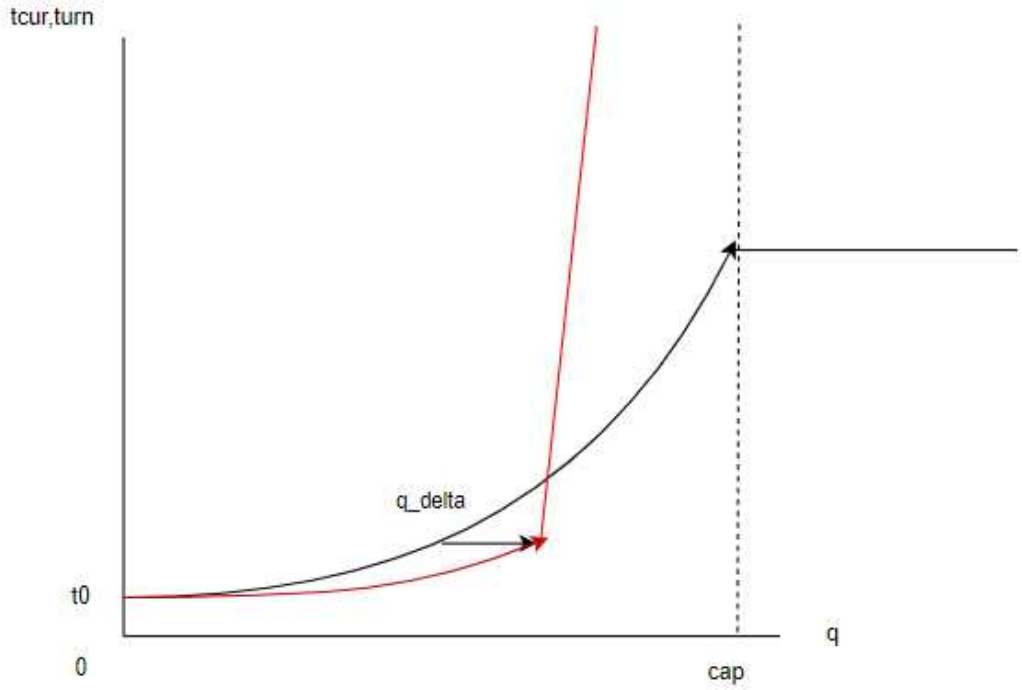

Figure 11: Link VDF modifications

The queuing effect is a linear graph that was found in section 2.2.2 as

$$t_{cur,BB} = \frac{\frac{I}{2}}{q_{eff}^{i}}\left(Q_{queue}^{i}\right) \tag{52}$$

Because queues and congestion heavily contribute to additional delay, this particular VDF has a very steep slope. Combining the modifications with the initial link VDF ends up with the new VDF shown in equation 53.

$$t_{cur,link} = t_0 * \left(1 + a * \left(\frac{q_{eff}}{cap * c}\right)^{b}\right) + \frac{\frac{I}{2}}{q_{eff}}\left(Q_{queue}^{i}\right) \tag{53}$$

For links that do not have a queue, the VDF equation becomes

$$t_{cur,link} = t_0 * (1 + a * \left(\frac{q - q_{delta}}{cap * c}\right)^{b} \tag{54}$$

3 Methodology

This section describes the methods, tools, and approaches used for the analysis. First, the software used for conducting the research is thoroughly explained. Currently, the ICA assignment is only implemented in the software used. Therefore, the knowledge and information needed to use the ICA assignment in the software is collected through meetings as described in the following chapter. Then, the stability assessment framework is presented, which is used to evaluate the stability of the ICA assignment. Accordingly, the procedure of the analysis in two case studies is elaborated. The first case study is an elementary network used to validate the problem of instability of the ICA assignment. On top of that, the elementary network contains very few elements and is committed to tracking the convergence

behavior of the ICA assignment as well. Besides, a real-life case study is developed and used to investigate the impact of different parameter settings on the stability of the ICA assignment. Also, the effect of the intersections calculated with the ICA is examined.

3.1 Software

3.1.1 PTV Visum

An implementation of the ICA assignment has been realized in the traffic modeling software Visum, developed by the PTV group. Visum is the world's leading transport planning software and is developed to assist transport planners and modelers in macroscopic modeling and simulations (Planung Transport Verkehr GmbH, 2024). It contains a variety of traffic assignments that are built into the software. Furthermore, it has a built-in function of the ICA assignment. Visum features a network editor and junction editor which can be used to develop networks and intersections, respectively. In Figure 12, the general window with the network editor is shown.

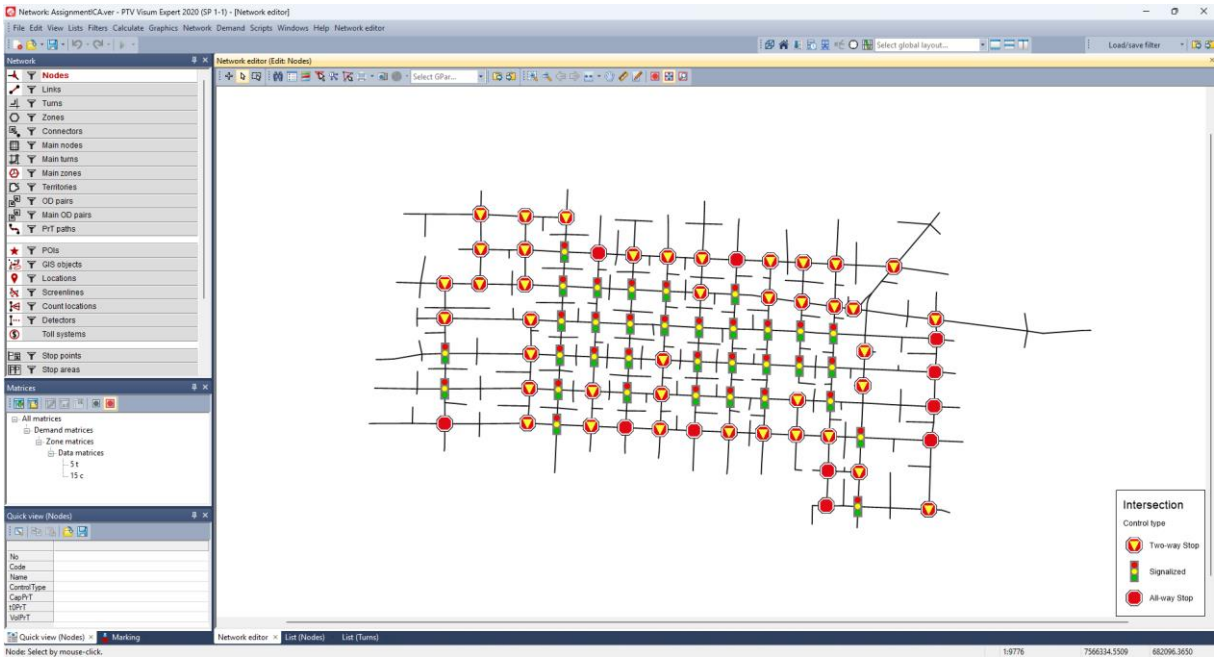

Figure 12: Network editor in Visum with an example network

The network shown is an arbitrary network provided within the installation of Visum. A clear distinction is made between each type of intersection with the assigned characters.

In a separate window, the 'Procedure sequence', procedures can be executed. This includes the operation of the ICA assignment alongside initialization and updates of features and results. In Figure 13, an example is shown of the Procedure sequence window. The procedure 'PrT Assignment' at line 1007, executes a traffic assignment. Visum offers a selection of various traffic assignments including the ICA assignment.

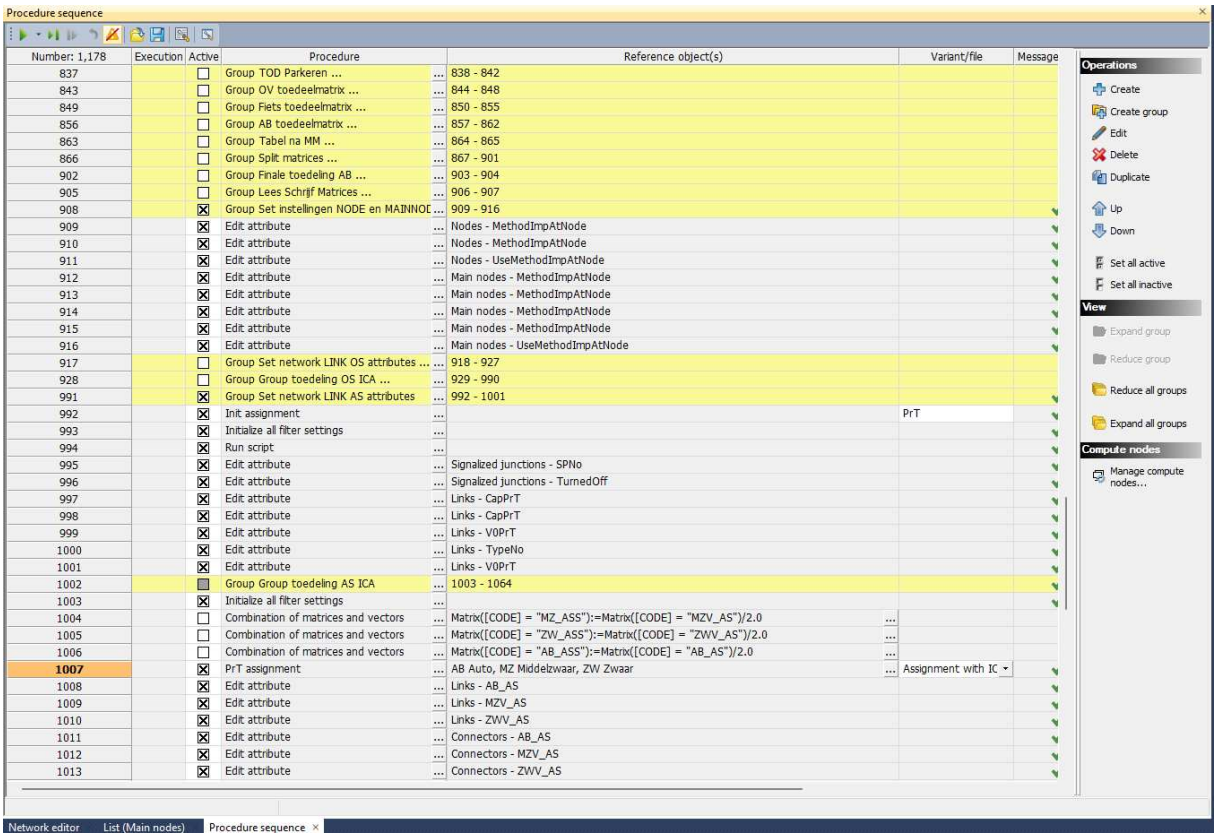

Figure 13: Procedure sequence window in Visum

3.1.2 Python

In this thesis, an in-depth analysis of the ICA assignment is carried out in Python, a programming language known for its good accessibility as an open source. Another reason that marks Python's convenience is the possibility of interacting with Visum. Visum includes a built-in Python interpreter that allows operations from a Python console. Furthermore, it is possible to use an external Python environment to open the Visum version file. After a version file is opened throughout Python, Visum modeling practices can be executed by invoking the applicable objects. On top of that, Python is used to transfer the results obtained to data storage in Excel.

3.2 Meetings and interviews

The ICA assignment in Visum is recognized as a complex process, that requires further investigation next to the available literature. Hence, several meetings and interviews were conducted next to a literature search for the successful implementation of the model. There are

At first, meetings with experienced Visum users from consultancy company Sweco were organized to improve understanding of the software's capabilities. These people have used Visum for many years in their projects resulting in a wide knowledge of the software. The meetings were used for the construction of networks and junctions and the execution of an ICA assignment. All in all, these sessions were valuable in speeding up the process and gaining a foundation for the modeling in Visum.

Despite this, extensive knowledge about the ICA assignment was still limited. Therefore, an additional online interview was arranged with a coworker of Sweco in the United Kingdom. She has used the ICA assignment in various projects. Hence, she has enriched experience with the ICA assignment in Visum, and was willing to share the success rates and limitations of the ICA assignment application as a tool in their projects.

To complement the theory behind the ICA assignment, an additional source of information was necessary. Therefore, a coworker at the PTV group was approached and requested to share more details about the theory behind the ICA assignment. This approach provided a general thesis description, emphasizing the instability issue in the ICA assignment. Because PTV is the founder of the ICA assignment, this gave reason to inform a technical specialist of the ICA assignment. An interview with the specialist was conducted to explain the observed problem in more detail and ask ICA assignment-related questions. The outcome of this meeting was beneficial, as it clarified the missing understanding of the ICA assignment. The technical specialist forwarded an explanation video about all steps in the ICA assignment. With the video and the Visum manual, the theoretical framework about the ICA assignment could be established. The technical specialist explained how ICA methodologies integrate with broader traffic system analyses and shared useful tips for the ICA assignment calibration. These tips were particularly effective during the development of the elementary network. Because this is a fictive network from scratch, mistakes were avoided which could lead to meaningless results. By emphasizing the urgency of the instability problem, the specialist was willing to help in the problem validation process by excluding certain causes and improving the components of the elementary network.

3.3 Elementary network

3.3.1 Description

An elementary network is developed to validate the problem and demonstrate instability occurring in a small network. This network is depicted in Figure 14.

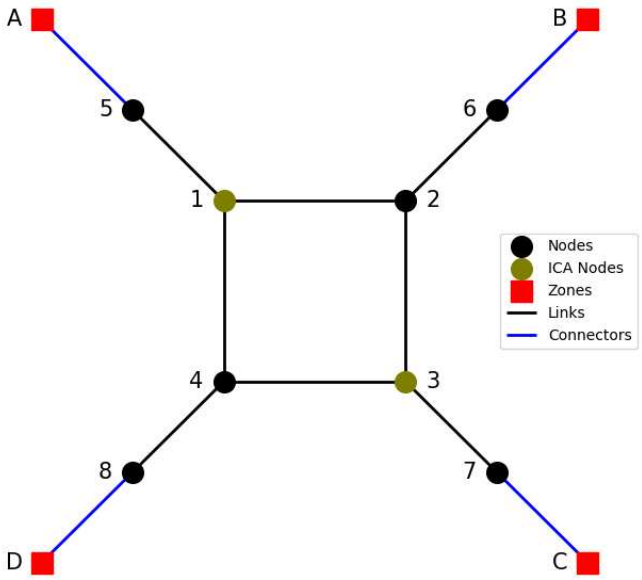

Figure 14: Graph model elementary network

The network contains 4 zones such that $\mathcal{Z} = \{A, B, C, D\}$ and 8 nodes $\mathcal{N} = \{1,2,3,4,5,6,7,8\}$. Within the set of nodes, 2 signalized intersections and delays will be calculated according to the ICA procedure. As discussed in Section 2, signalized intersections subdue more delay variations, highlighting the need for precise delay estimations. Therefore, the ICA is adopted on signalized intersections only. Hence, nodes 1 and 3 are signalized intersections calculated with the ICA, displayed in olive. The other 6 nodes displayed in black have delays and capacities captured as a constant value. Furthermore, 8 links connect the nodes, and 4 connector links in blue connect the zones to the nearest node. The travel time for each link is described with the same VDF shown in equation 55.

$$t_{cur} = t_0 * \left(1 + a * \left(\frac{q}{q_{max} * c}\right)^b\right) \quad 55$$

The traffic flow is observed after allocating traffic demand between zones A and C. Traffic demand travels from zone A to C; no demand travels in the opposite direction. As a result, the traffic is submitted to choose between two possible routes:

- R1: A->5->1->2->3->7->C
- R2: A->5->1->4->3->7->C

The elementary network structure has been designed to ensure that all routes have roughly equivalent impedance, making them equally attractive. This design aims to effectively manage the increase in demand between zones A and C. Specifically, when an additional vehicle opts for R1, the impedance on R1 increases, making R2 more attractive for the next vehicle. Consequently, as vehicles switch between R1 and R2, the impedance on both routes will gradually increase, resulting in a balanced traffic flow.

All intersection nodes contain a more detailed design than provided in the graph network in Figure 14. On top of that, the ICA nodes need to have all input variables defined, which are required for the ICA. The geometry of the ICA nodes is shown in Figures 15 and 16, for nodes 1 and 3 respectively.

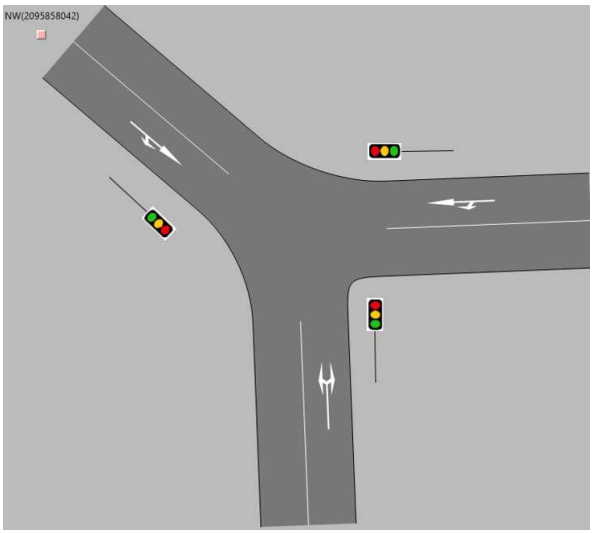

Figure 15: Intersection design of ICA node 1

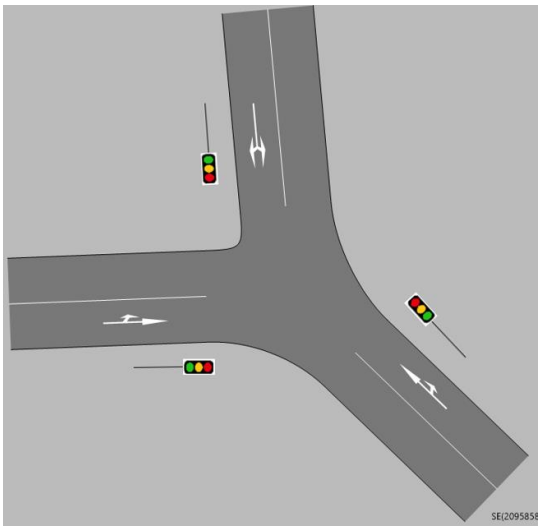

Figure 16: Intersection design of ICA node 3

The design is simple, where each direction has one incoming lane. As a result, the traffic coming from a northwestern direction in Figure 15, consists of movement groups in eastern and southern directions.

A signal phasing plan has been developed for both intersections, which include three incoming lanes. Given that all lanes are shared, three traffic lights are required at each intersection. The plan allocates 30 seconds of green time for each direction in every phase, with an additional 1-second interval between the phases. Consequently, this configuration results in a total cycle time of 93 seconds for both intersections.

3.3.2 ICA assignment analysis

This section outlines the methodology employed to investigate the instability issues within the assignment. The analysis focuses on the impact of varying traffic demands between zones A and C on total traffic volume and impedance, and how these factors influence the stability and convergence of the ICA assignment.

To systematically explore the instability, traffic demand scenarios are modeled from 0 to 2000 vehicles, with increments of 10 vehicles per scenario. This approach generates a comprehensive set of 200 distinct traffic scenarios, allowing for a detailed examination of how different levels of demand influence the impedance and traffic dynamics in the network.

In addition to analyzing impedance and traffic volume, the convergence behavior of the ICA assignment is observed. This is done for all selected subordinate assignments in the ICA assignment. The goal is to identify the conditions that cause a potential slower convergence. In a stable traffic assignment, the algorithm should converge consistently irrespective of the initial situation. Therefore, there is a strong relationship between the conditions that do not reach convergence and the stability of the ICA assignment. A condition is fulfilled when its threshold value is exceeded. These conditions must be met for a user-defined share of links or turns. The threshold and share values for each condition are shown in Table 17 in Appendix E and are based on the standard values from the Visum manual. (PTV Group, 2023). The last condition considering queue differences is solely bounded to a threshold value and not to the share of links on which the queue lengths are formed.

3.4 Real-world network

Next to the elementary network, a real-world network case study is established. With a real-world network, empirical data reflect the details and complications of actual traffic situations. By applying this research to a real-world network, the obtained results and insights can be used for similar scenarios elsewhere. Furthermore, a case study considers a complete set of variables in the context of transportation systems. This avoids problems of overlooking certain variables in hypothetical cases such as the elementary network.

In this section, a description of the real-world study area is given. Then, the data needed for the model is described. With that information, the methodology of the ICA intersection analysis is explained.

3.4.1 Description

The case study area is located in Utrecht, the Netherlands. Utrecht is one of the largest cities in the country with a population of 367.947 (CBS, 2023). Because of its centralized position and high level of urbanization, Utrecht is exposed to high traffic volumes that travel in, out, and through the city. Due to this, the challenges related to traffic congestion are a daily recurring phenomenon.

Within the limitations of accessible data sources, the upper part of the city is selected as the final study area. These locations are the districts shaded in green as depicted in Figure 17. A further explanation of the used data is given in the next section.

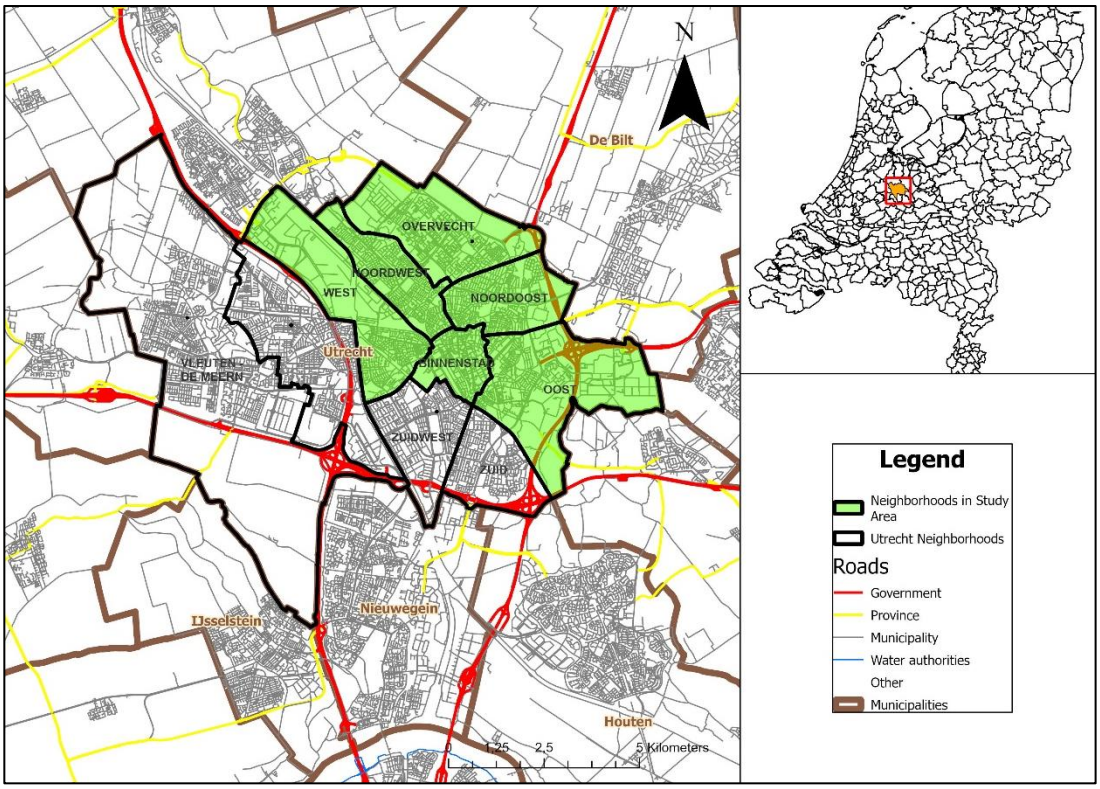

Figure 17: Overview of the study area

3.4.2 Data

The data required for this thesis is provided by the consultancy firm Sweco. This dataset consists of the traffic network and the required traffic demand stored in OD matrices calibrated to the values observed in the real world. This is sufficient information to carry out a traffic assignment and predict the traffic flows in the municipality of Utrecht.

3.4.2.1 Traffic network

An overview of the present network items is given in Table 6.

Table 6: Real-world network objects

Item	Type	Value
Nodes	Uncontrolled	1711
	Signalized	33
	Two-way yield	233
	Unknown	4762
Main nodes	Signalized	48
	Two-way yield	35
	Roundabout	13
Links (directed)		18762
Zones		266
Turns		57262

In the network, a distinction is made between nodes and main nodes. The main nodes are the larger intersections with a high number of incoming lanes, typically experiencing higher traffic volumes compared to standard nodes. Both are categorized into subtypes based on their geometric characteristics. The categories are uncontrolled, signalized, two-way yield, and roundabout. Furthermore, multiple nodes do not fall into any category and are scaled under unknown. The network as developed in graph

theory is shown in Figure 18. All signalized intersections are depicted with the traffic sign, adding up to 81 in total.

Out of all signalized intersections, only a limited amount can be used for the ICA. Because the procedure of ICA has many input variables, an intersection in which delay and capacity are calculated with ICA requires an adequate level of detail. In other words, the signalized intersections need to be modeled correctly to use them for the ICA. Most intersections fail to meet the necessary criteria due to missing signal phasing data. This is a data limitation because actual intersections usually have a phasing plan. Nevertheless, 23 signalized intersections meet the requirements for the ICA calculations, as illustrated in Figure 19. Of these, 17 intersections are classified as main nodes, while 6 are considered regular nodes. To analyze stability in the network, these intersections will all be utilized to calculate capacity and delay using ICA.

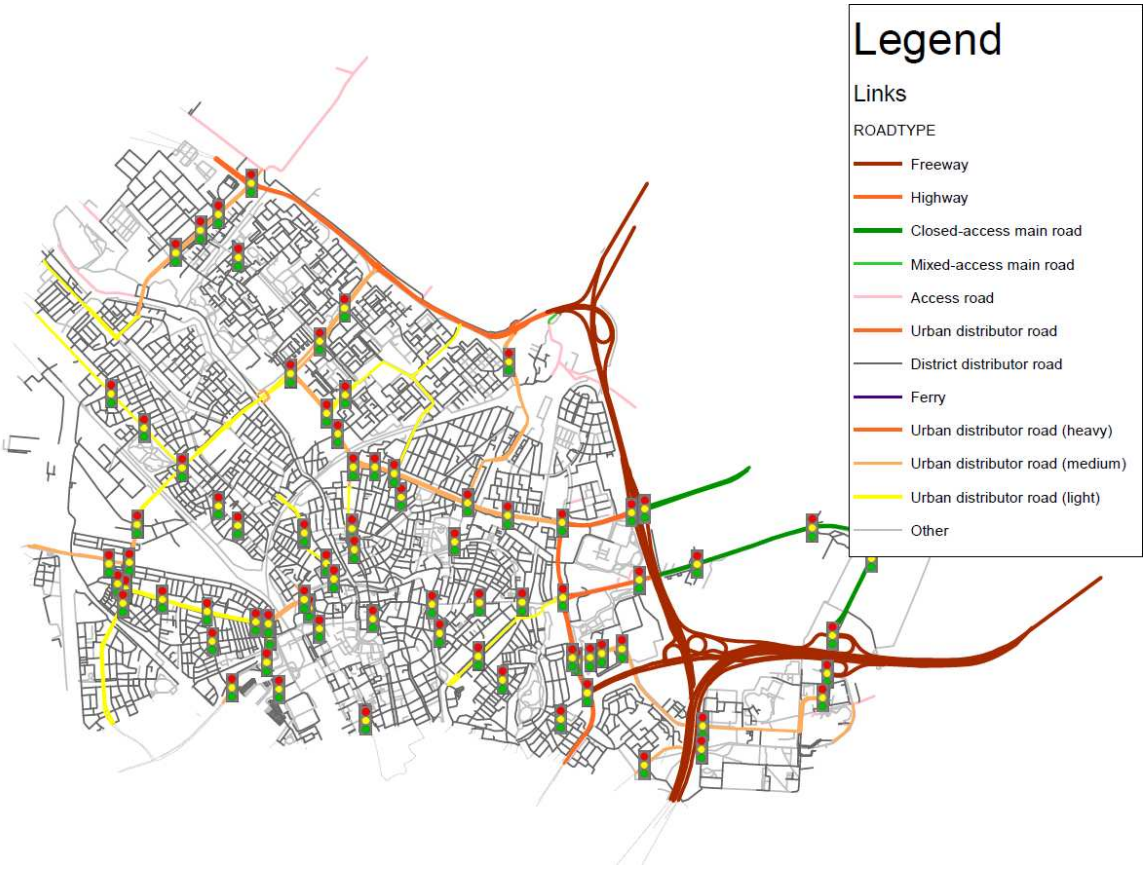

Figure 18: Graph network of the study area

Figure 19: Signalized intersections suitable for the ICA

In the elementary network, only 2 zones were employed for traffic demand. In this case, the entire network is divided into 266 distinct zones that serve as the starting points and endpoints for the traffic demand. As depicted in Figure 20, there are 154 zones within the defined study area. The zones that fall outside the study area are referred to as cordon zones, of which there are 96 in total. Cordon zones are situated at the network edge, closest to their real-world locations. Additionally, 16 zones are allocated to represent parking areas and public transport facilities.

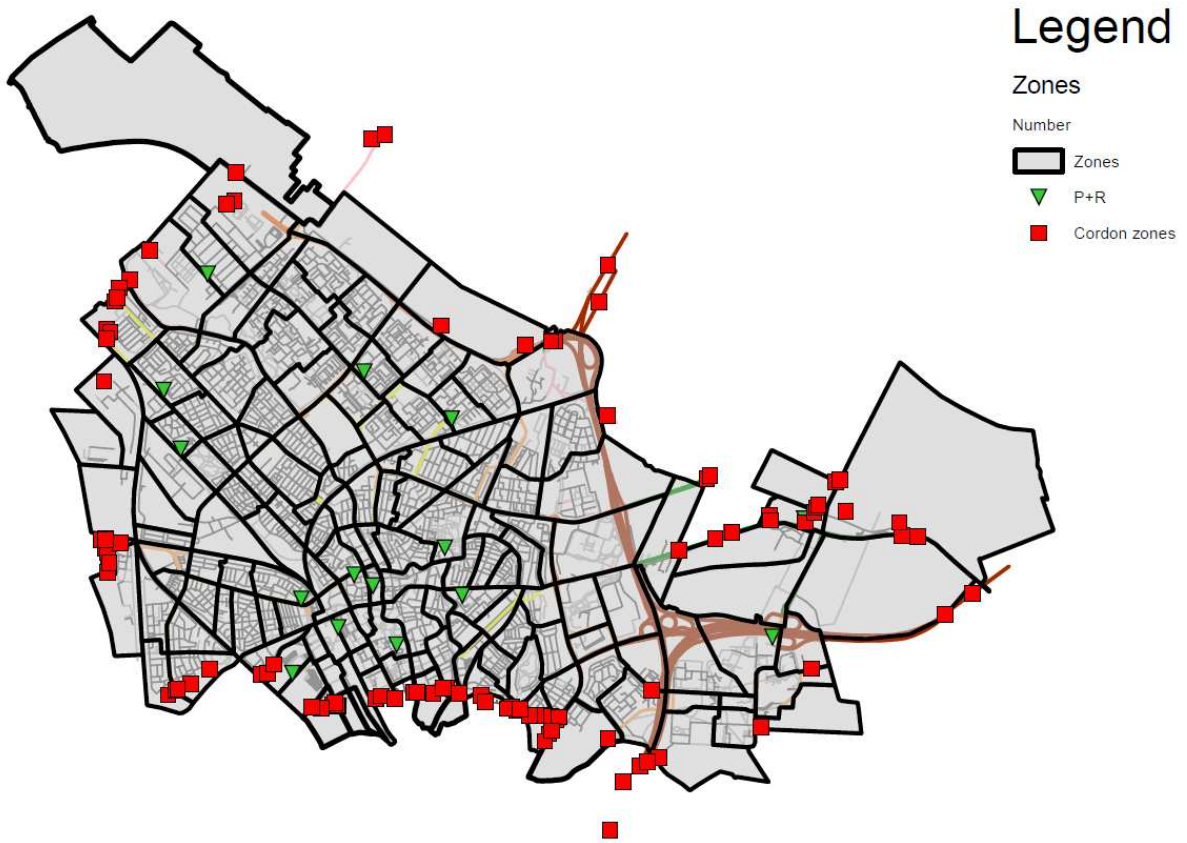

Figure 20: Zones in the study area

3.4.2.2 OD-matrix

The traffic demand across the zones is represented in three OD matrices: one for cars, one for medium-weight vehicles, and one for heavy-weight vehicles. Traffic counts determine the traffic demand and have been retrieved through three sources. First, the counts on local roads were executed by VervoersRegioUtrecht (VRU) in 2015. The second part contains the counts for province roads in 2017. These were conducted by the Nationaal Dataportaal Wegverkeer, a Dutch instance that manages traffic and road data. The last counts have been derived from INWEVA which consists of highways and motorways, also measured in 2017. All counts have been measured during the evening peak and are adapted to meet hourly intensities. In Table 7, descriptive statistics are shared about the demand data.

Table 7: Demand data descriptive statistics

		Origin trips generated (veh/hour)	**Destination trips generated (veh/hour)**
Cars	Total trips	24930.0	30177.8
	Mean	0.352	0.427
	Median	0	0
	Maximum (1 zone)	2807.7	1803.2
Medium-Heavy	Total trips	894.7	1067.5
	Mean	0.013	0.015
	Median	0	0
	Maximum (1 zone)	218.7	103.6
Heavy	Total trips	916.7	939.4
	Mean	0.013	0.013
	Median	0	0

	Maximum (1 zone)	547.0	243.4

3.4.3 Intersection analysis

A part of the case study on the real-world network is the influence of the selected intersections to be calculated with ICA. In the impact analysis of input parameters, all intersections suitable for ICA will be calculated with ICA. However, their location and quantity might also impact the stability of the ICA assignment. Therefore, an intersection analysis is set up to investigate the influence of the specific intersections calculated with ICA. The effect on the stability is studied with two different intersection analyses. First, the location of the ICA intersections is investigated by establishing the stability of the ICA assignment for each ICA intersection separately. Because there are 23 intersections suitable for ICA, 23 alternatives are considered. For each, the stability is then calculated for a comparative scenario with one ICA intersection.

Subsequently, the quantity of ICA intersections is examined by developing another 23 alternatives. Based on the outcome of the single ICA intersection analysis, the intersections are sorted based on their stability outcome. Then, the stability is determined for 23 alternatives in which the number of ICA intersections is incremented according to the sorted list. As a result, the alternatives consist of 1, 2 to 23 intersections that are calculated with ICA, respectively. The latter analysis aims to examine the influence of equipping more intersections with ICA on the stability of the ICA assignment. For both analyses, the default configuration of the ICA assignment is used as explained in Table 18 in Appendix F.

3.5 Stability assessment framework

Because stability can be a vague concept, a meaningful framework for the assessment is essential. This framework contains the methodology for determining stability in the experiments to parameters as explained in section 3.6. On top of that, stability is defined such that it can be applied on all types of networks and is deployable in different situations. The definition of stability in this study follows the definition as researched in the work of Lu & Nie (2010). A model is stable when small perturbations of input values lead to small changes in the solution. Furthermore, Lu & Nie (2010) researched the stability of a route-based equilibrium assignment also known as the gradient projection method. They assessed the stability based on the change in traffic after three perturbed scenarios. These perturbations represent a small approximation error in free flow speed, capacity, and OD demand, respectively. The scenario of changing the OD demand is used to activate the stability issues in this work. The origin of the instability problem has been identified by changing the OD demand with a slight value. Therefore, this perturbation scenario is ensured to contain the problem that occurs.

Assessment of traffic changes can be done on either route or link level. In the literature on transportation and traffic flow, it is recognized that even when a unique traffic equilibrium state is reached, the specific paths chosen by travelers may vary (Sheffi, 1985). Despite the variability in individual route selection, the cumulative traffic flow on each link in the network aligns with the unique equilibrium condition. Using route flows might give a more accurate result in measuring stability, because of its higher detail. However, its use for analysis is limited in literature and encounters increasing complexity when examining stability in larger networks. Hence, only link flows are considered in the stability assessment framework. The stability is assessed on link level by comparing the assignment result of a base scenario with a perturbed scenario. The perturbed scenario concerns the value between a single OD-pair, such that the entire perturbed matrix is nearly identical to the base scenario OD-matrix.

The stability of the network is determined in two ways. First, an absolute measure is used that reflects the change of traffic in the network as a response to the perturbation. This measure is determined as the number of links that have changed due to the perturbation with at least a traffic volume of 1 vehicle.

The total number of links that satisfy this condition is divided by the total number of links in the network such that it contains a value between 0 and 1. In Equation 56, the measure is elaborated.

$$S_1 = \frac{1}{|\mathcal{L}|}\sum_{l=1}^{\mathcal{L}} 1\left(\left|q_l^{base} - q_l^{perturbed}\right| \geq 1\right) \quad 56$$

The second measure is based on the relative error between the perturbed scenario and the base scenario. This will take the exact volume changes at each link into account. By dividing the difference at each link with the volume of the base scenario a relative error is computed. Then, adding the relative errors for each link and dividing by the total number of links returns the average relative error in the entire network. However, there will always be a small error due to the applied perturbation on purpose. Therefore, this guaranteed error is subtracted from the relative error to get the true average relative error. The guaranteed error is defined as the minimum error upon the perturbed scenario. An impedance-based shortest path search returns the smallest error possible, where the perturbation is the demand traveling the shortest path. Therefore, the guaranteed error is presented by the sum of perturbed demand at the shortest path links between the concerned OD pair. Next to the average relative error, the maximum relative error is computed as well. This is the maximum of all relative errors and is used as an indicator of the magnitude of the error. The stability indexes S_2^{RE}, S_2^{ME} for the average relative error and maximum relative error are displayed in Equations 57 and 58, respectively.

$$S_2^{RE} = \frac{1}{|\mathcal{L}|}\sum_{l=1}^{\mathcal{L}} \frac{|q_l^{base} - q_l^{perturbed} - \Delta q_{dem,l,SP(ij)}|}{q_l^{base}} \quad 57$$

$$S_2^{ME} = \max_{all\ l \in \mathcal{L}} \left(\frac{|q_l^{base} - q_l^{perturbed} - \Delta q_{dem,l,SP(ij)}|}{q_l^{base}}\right) \quad 58$$

Where, q_l^{base} the volume in the base scenario on link $l \in \mathcal{L}$, $q_l^{perturbed}$, the volume in the perturbed scenario on link $l \in \mathcal{L}$ and $\Delta q_{dem,l,SP(ij)}$ the demand perturbation traveling the shortest path on links $l \in \mathcal{L}$ between origin zone $i = A$ and destination zone $j = C$.

For both instances an assumption is involved such that the outlying values are avoided. Each term is only calculated for links that satisfy

$$q_l^{base} \geq 0.1 \quad 59$$

Without this constraint, links with minimal demand cause disproportionately large relative errors, despite the absolute differences being small. Links that do not meet this constraint are assigned with zero error.

The stability measure is used in the experiments that are executed in both networks. For a stability analysis, the base scenario and perturbed scenario must be determined. The perturbed scenario is defined by increasing the demand between a single OD pair. In the next two subsections, the procedure for selecting the base scenario and perturbed scenario is explained for both networks.

3.5.1 Elementary network

In the elementary network, deployment of the stability indices works slightly differently as proposed in the previous section. Since there is only one OD-pair containing demand, this OD-pair is used for the perturbed scenario. However, this allows for one analysis result which is insufficient for the experiments. As previously discussed in subsection 3.3.2, an analysis of the ICA assignment is done in the elementary network, by allocating different traffic demands between zones A and C. This analysis contains 200 scenarios where the traffic demand in each scenario is arranged such that

$$q^{i}_{dem,AC} \in \{0, 10, 20, 30, \dots., 1980, 1990, 2000\}$$

Where $q^{i}_{dem,AC}$ is the demand of scenario $i \in \{0,1,2 \dots,200\}$ between zone A and C.

Hence, the stability indices can be determined for the same 200 cases as used in the ICA assignment analysis. However, scenarios containing demand smaller than 200, experience unequal impedances of the routes, since they are not identical. The impedance of both routes is brought after some demand is assigned to the network. Therefore, a warmup time is needed to ensure that the impedances of both routes are the same. To be sure that the warmup time is not included in the scenarios of the stability analysis, the scenarios are taken between values of 1000 and 2000 demand. The scenarios for the stability analysis then consist of demand values between this interval. The demand for perturbed scenario i, serves as the base scenario for the next perturbed scenario $i+1$. Subsequently, the perturbed scenario $i+1$ serves as base scenario for perturbed scenario $i+2$, and so on. In Table 8, an overview is given of the existing base and perturbed scenarios in the elementary network.

Table 8: Stability scenarios in elementary network

$q^{base,i}$	$q^{base,1}$	$q^{base,1}$	...	$q^{base,199}$	$q^{base,200}$
$q^{base,i}_{dem,AC}$	1000	1005	...	1990	1995
$q^{perturbed,i}$	$q^{perturbed,0}$	$q^{perturbed,1}$	...	$q^{perturbed,199}$	$q^{perturbed,200}$
$q^{perturbed,i}_{dem,AC}$	1005	1010	...	1995	2000

Because the elementary network is imaginary, it does not violate any calibrated parameters about the prediction of reality. And, due to its simplicity, many ICA assignments can be executed within a short amount of time. Therefore, a stability analysis of 200 scenarios is feasible.

The number of links in the network that are traveled through the scenarios is six in total. Because of this, the first stability index that computes the proportion of links that have at least a difference of 1 vehicle is omitted. For the second stability index, the minimum error in the relative error equations is determined differently for the situation when congestion occurs in the network. This happens when demand is higher than the capacity of the first encountered intersection. Vehicles will queue on the link upstream and there are no more increasing traffic volumes on the links downstream. Hence, the minimum error in the oversaturated case must take the queuing vehicles into account. Moreover, the shortest path search for finding the minimum error is now infeasible because the perturbated demand is not expected to make the trip between zones A and C. Therefore, the relative error stability must be adapted when the network reaches congestion. In Equations 60 and 61, the stability index calculations $S_2^{RE,i}$ and $S_2^{ME,i}$ for scenario i is shown for the free flow and congested state, based on the condition of queue existence in the network.

$$S_2^{RE,i} = \begin{cases} \frac{1}{|\mathcal{L}|} \sum_{l=1}^{\mathcal{L}} \frac{|q_l^{base,i} - q_l^{perturbed,i} - \Delta q_{dem,l,SP(AC)}|}{q_l^{base,i}} \; if \; Q_{queue,l}^{base,i} = 0 \\ \frac{1}{|\mathcal{L}|} \sum_{l=1}^{\mathcal{L}} \frac{|q_l^{base,i} + Q_{queue,l}^{base,i} - q_l^{perturbed,i} - Q_{queue,l}^{perturbed,i} - \Delta q_{dem,c,AC}|}{q_l^{base,i} + Q_{queue,l}^{base,i}}, \; else \end{cases} \quad (60)$$

$$S_2^{ME,i} = \begin{cases} \max_{all\ l \in \mathcal{L}} \frac{|q_l^{base,i} - q_l^{perturbed,i} - \Delta q_{dem,l,SP(AC)}|}{q_l^{base}} \; if \; Q_{queue.l}^{base,i} = 0 \\ \max_{all\ l \in \mathcal{L}} \frac{|q_l^{base,i} + Q_{queue,l}^{base,i} - q_l^{perturbed,i} - Q_{queue,l}^{perturbed,i} - \Delta q_{dem,c,AC}|}{q_l^{base,i} + Q_{queue,l}^{base,i}}, else \end{cases} \quad (61)$$

Where $Q_{queue,l}^{base,i}$, the queue in the base scenario on link $l \in \mathcal{L}$, $Q_{queue,c}^{base,i}$, the queue in the base scenario on congested link $c \in \mathcal{L}$, $Q_{queue,l}^{perturbed,i}$, the queue in the perturbed scenario on link $l \in \mathcal{L}$, $Q_{queue,c}^{perturbed,i}$, the queue in the perturbed scenario on congested link $c \in \mathcal{L}$ and $\Delta q_{dem,c,AC}$ the demand perturbation ending up on congested link $c \in \mathcal{L}$. Then, the final relative error is the maximum of the relative error in the scenarios, as shown in Equations 62 and 63. In this way, the worst stability outcome of all scenarios is captured.

$$S_2^{RE} = \max_{all\ i} S_2^{RE,i} \tag{62}$$

$$S_2^{ME} = \max_{all\ i} S_2^{ME,i} \tag{63}$$

3.5.2 Real-world network

The stability indices can be applied to the real-world network by changing the demand $\Delta q_{dem,ij}$ between a particular zone $i \in \mathcal{O}$ and $j \in \mathcal{D}$ and compare the results of the two scenarios. Since there are 70.756 OD pairs, investigating all of them in the stability measure is infeasible. Therefore, a sample from these OD-pairs is selected which serves as a representation for all OD-pairs in the region. To develop a well-grounded sample set, zone pairs are selected based on two factors. At first, the traffic demand that exists between two zones must be greater than 0. This avoids the emergence of an unrealistic scenario of zone-pairs with no demand suddenly containing demand. With the remaining OD-pairs, the Euclidean distance is used as the second factor. All OD-pairs are sorted based on their Euclidean distance. From these, a selection of 20 OD-pairs is made, in which a variety of different distances is considered. This is done by choosing every mth OD-pair such that 20 OD-pairs $ij \in \mathcal{O}, \mathcal{D}$ are selected as shown in equation 64.

$$ij = m * \frac{|\mathcal{O}_{>0} * \mathcal{D}_{>0}|}{|M|}, \forall m \in M \tag{64}$$

The nominator presents the sorted list of OD-pairs with positive demand and $M = \{1, 2, \dots, 20\}$ the set of scenarios. It is assumed that 20 OD-pairs give a sufficient view of the stability of the entire network and the computational effort is acceptable within the given timeframe. Then, the first stability index S_1^m for a scenario m, where a perturbation is applied to the demand between origin i and destination j is calculated with

$$S_1^m = \frac{1}{|\mathcal{L}|} \sum_{l=1}^{\mathcal{L}} 1\left(|q_l^{base,m} - q_l^{perturbed,m} - \Delta q_{dem,l,SP(ij)}| \geq 1\right) \tag{65}$$

The second stability index couple S_2^{RE} and S_2^{ME} for a scenario m are calculated with

$$S_2^{RE,m} = \frac{1}{|\mathcal{L}|} \sum_{l=1}^{\mathcal{L}} \frac{|q_l^{base,m} - q_l^{perturbed,m} - \Delta q_{dem,l,SP(ij)}|}{q_l^{base,m}} \tag{66}$$

$$S_2^{ME,m} = \max_{all\ l \in \mathcal{L}} \left(\frac{|q_l^{base,m} - q_l^{perturbed,m} - \Delta q_{dem,l,SP(ij)}|}{q_l^{base}}\right) \tag{67}$$

Instead of taking the maximum of all scenarios, the average is chosen in the real-world network. This is done because the sample size is significantly lower than in the elementary network. Furthermore, it is

valuable to include the outcomes of all scenarios for this case. Thus, the average and maximum relative error is calculated with

$$S_2^{RE} = \frac{1}{|M|} \sum_{m=1}^{|M|} S_2^{RE,m} \quad 68$$

$$S_2^{ME} = \frac{1}{|M|} \sum_{m=1}^{|M|} S_2^{ME,m} \quad 69$$

Based on the outcomes of the average relative error S_2^{RE}, a score Table 9 has been developed to enhance the meaning of each error. The score ranges from 1 to 10, with 1 indicating very unstable and 10 completely stable.

Table 9: Stability scores

Average relative error	Stability Score
$\boldsymbol{S_2^{RE} < 0.001}$	10
$\boldsymbol{0.001 \leq S_2^{RE} < 0.002}$	9
$\boldsymbol{0.002 \leq S_2^{RE} < 0.003}$	8
$\boldsymbol{0.003 \leq S_2^{RE} < 0.004}$	7
$\boldsymbol{0.004 \leq S_2^{RE} < 0.005}$	6
$\boldsymbol{0.005 \leq S_2^{RE} < 0.006}$	5
$\boldsymbol{0.006 \leq S_2^{RE} < 0.007}$	4
$\boldsymbol{0.007 \leq S_2^{RE} < 0.008}$	3
$\boldsymbol{0.008 \leq S_2^{RE} < 0.009}$	2
$\boldsymbol{S_2^{RE} \geq 0.009}$	1

3.6 Experiment setup

With the defined stability assessment framework, several experiments are executed in both the elementary and the real-world network. In each experiment, one parameter setting is investigated. This particular parameter value is changed and the corresponding stability indices are calculated. Eventually, the stability results are compared to examine the differences. The goal of these experiments is to identify the impact of each parameter on the stability of the ICA assignment. Based on the contents of the theoretical framework and the possibilities for alternative parameter configurations in the ICA assignment, the parameters determined for the experiments are shown in Table 10. It are all model-related parameters, that are applied in different stages of the ICA assignment.

Table 10: Examined ICA assignment parameters in experiments

Stage	Parameter name	Description
Blocking back model	SmoothingFactor	Smoothing factor used to smooth the turn volumes resulting from blocking back
Initialization	InitCapSharedLanes	Initial capacity of lanes at shared lanes
Blocking back model	UseBBackLinkCap	Option to use link capacities on top of turn capacities in the blocking back model

Blocking back model	BBackCalculationVariant	The type of blocking back algorithm used.
Blocking back model	BBackNumberOfVolumeSlices	Number of slices in which the blocking back model distributes traffic volume over the network
Subordinate assignment	MaxGap	Relative gap between the final result and its predecessor
Subordinate assignment (LUCE)	MeshProportionalityOptimizationMode	Optimization of proportionality in route volumes at network objects

Some parameters have not been mentioned in the theoretical framework and need some further explanation. First, the InitCapSharedLanes parameter defines the method by which capacity at shared lanes is determined. This can be based on the full capacity such that each turn or traffic movement using the shared lane is assumed to have access to the full capacity of the lane. Another possibility is that the capacity of the shared lane is divided among the different turns or movements. The latter option causes the shared lanes to reach capacity faster. Hence, congestion is expected to occur more often. Because congestion effects may influence the stability of the ICA assignment, this parameter must be considered. Second, UseBBackLinkCap offers the possibility to incorporate link capacities in the blocking back model. By default, the blocking back model considers the capacity of turns only. With the link capacities considered as well, more congestion will emerge. Third, the BBackCalculationVariant contains two different procedures for the execution of the blocking back model. The difference between them is the exploitation of capacity over the routes. One procedure carries out this exploitation parallel to all routes whereas the other handles each route sequentially. At last, the MeshProportionalityOptimizationMode is distinctively available for the LUCE algorithm. This offers the opportunity to consider proportionality in the traffic assignment. If proportionality is considered, it can be achieved for all transport types together or separately. Since multiple transport types only exist in the real-world network, the MeshProportionalityOptimizationMode is investigated for this case study.

To execute the experiments a default scenario for the ICA assignment operating under the three subordinate must be developed. The parameter settings for the default scenario are based on the information provided by PTV and are shown in Table 11. Generally, the initial parameter values as stated in the ICA assignment model in Visum and as recommended in the Visum manual (PTV Group, 2023), form the settings for the default scenario. In the right column, the different values different from the default scenario are presented. In some instances, the options are presented in text. These instances are differentiated by an integer enclosed in parentheses behind it, which is used in Visum to refer to these alternatives.

Moreover, each experiment follows the same convergence settings as applied in the ICA assignment instability analysis in section 3.3.2. These can be found in Table 17 in Appendix E.

Table 11: Experiments (default and alternative values)

Parameter name	**Default**	**Tested values**
SmoothingFactor	0.7	0.56
		0.63
		0.77
		0.84
InitCapSharesLanes	Total capacity for each turn (1.0)	Shared capacity for each turn (0.0)

UseBBackLinkCap	Vehicles are blocked back based on turn capacities (0.0)	Vehicles are blocked back based on link capacities (1.0)
BBackCalculationVariant	Capacities are exploited evenly over all routes (0.0)	Capacities are exploited sequentially over all routes (1.0)
BBackNumberOfVolumeSlices	20	10
		30
		50
		100
MaxGap (BEA)	0.0001	0.001
		0.00001
MaxGap (BFW)	0.001	0.0001
		0.00001
MaxGap (LUCE)	0.00001	0.001
		0.0001
MeshProportionalityOptimizationMode (LUCE)	No proportionality (0.0)	Achieve proportionality for transport systems separately (1.0)
		Achieve proportionality for transport systems jointly (2.0)

The default value used for the smoothing factor is 0.7. This value came out as the most suitable value for smoothing the turn volumes after testing the ICA assignment (Planung Transport Verkehr GmbH, 2024). It is decided to compare four alternative values for the smoothing factor. These values are considered sufficient to examine the stability in a range of smoothing factors around the tested default value. Regarding the BBackNumberOfVolumeSlices, a default value of 20 is set. A larger number of slices ensures a more detailed distribution of traffic flow but requires more computational effort. In Visum, 100 slices is the maximum that can be used. Therefore, the values 10, 30, 50, and 100 are chosen to include a mixture of possible values for the number of slices. In each subordinate assignment, a MaxGap is used as explained in section 2.2. The default values as stated in the Visum manual are 0.0001, 0.001, and 0.00001 for BEA, BFW, and LUCE respectively. Although, the three selected subordinate assignments are relatively new developments, smaller gaps than 0.00001 require a lot of computational effort. Because the subordinate assignment is repeatedly executed in the ICA assignment, even more computation time is required. Moreover, the stability calculation consists of 200 and 20 scenarios in the elementary and real-world networks, respectively. Therefore, the consideration of a gap smaller than 0.00001 is beyond the scope of this research and alternative gaps of 0.001, 0.0001, and 0.00001 are established.

4 Results

This section presents the findings derived from the comprehensive analysis conducted on both the elementary and real-world networks using the ICA assignment as implemented in Visum. Following the outlined methodology, this results section elaborates on the impacts observed from varying the parameters specified in the experimental setup and investigates the stability of the traffic assignments under different conditions.

4.1 Elementary network

4.1.1 ICA assignment instability validation

The instability of the ICA assignment is validated through the total impedance and traffic volume in the network for different traffic demands. In the graphs in Figure 21, the change in total impedance and traffic volume is shown on the left and right sides, respectively. From top to bottom, the three different subordinate assignments, BEA, BFW, and LUCE are depicted.

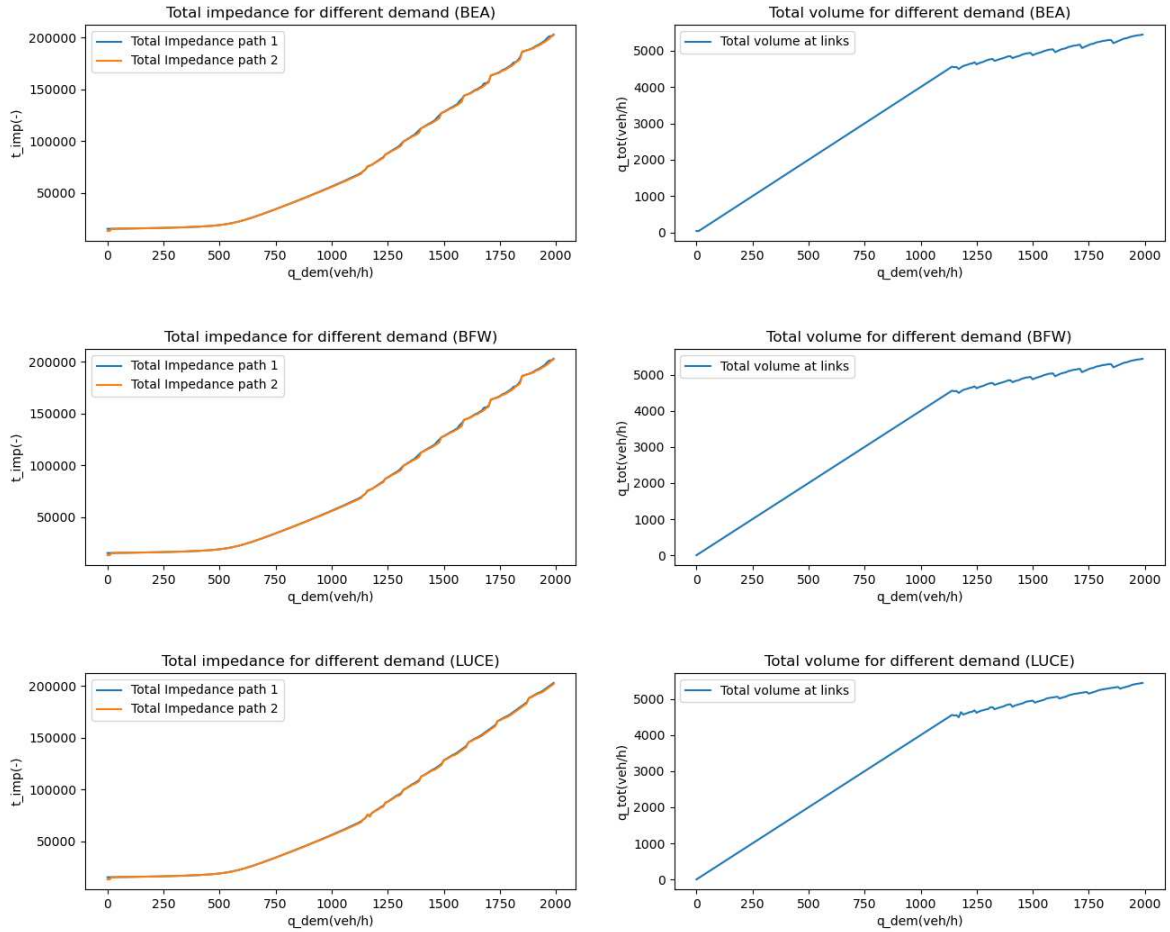

Figure 21: ICA assignment analysis to total impedance and total traffic volume (BEA, BFW, LUCE)

Regarding the graphs considering impedance on the left side, it stands out that for each subordinate assignment similar patterns occur. Furthermore, the impedance for paths 1 and 2 is consistently close to each other, as expected. Zooming in on the result of the total impedance of BEA, a linear increase of the impedance happens until a demand of 500 vehicles. Between 500 and 1100 vehicles it proceeds linearly but with a slightly steeper slope. This can be explained by the fact that the impedance is directly related to the link and turn VDFs which have an exponential curve. As a result, the total impedance grows faster for higher traffic demand. A the benchmark of 1100 vehicles the curve starts to oscillate. At this point, the ICA intersection at the top left has reached its capacity for letting traffic through in the eastern and southern directions. The capacity of the intersection is then calculated by the ICA as follows.

$$c_E + c_S = N_E * s_E * \frac{g_E}{C} + N_S * s_S * \frac{g_S}{C} = 1 * 1839 * \frac{30}{93} + 1 * 1740 * \frac{30}{93} = 1154.5\ veh/h$$

Therefore, the intersection reaches its capacity at a demand of 1154 veh/h. However, the blocking back model considers a slightly lower capacity than is calculated by the ICA. This effect has been

implemented to create a more realistic approach to queue development. In real-world scenarios, when vehicle flows start coming close to a capacity, queues already start to emerge. Hence, vehicles are stored in a queue before the actual capacity is reached. Based on the graphs of total traffic volume in Figure 21, the same oscillating pattern is observed for the total impedance. For a stable assignment, it is expected that impedance would increase linearly after demand reaches capacity constraints, with new demand accumulating in the queue. However, this does not occur, and the assignment yields varying results, which are depicted as the oscillating patterns in the graphs. The same is observed for the total traffic volume trial for different traffic demands. The traffic volume increases linearly until around 1150 veh/h, the capacity of the first intersection. After a demand of 1150 veh/h, it shows a similar oscillating pattern as for the total impedance although it is expected to grow linearly.

The oscillating pattern is examined in more detail by comparing two different traffic demands that only differ in one vehicle. In Figures 22 and 23, this is illustrated at a traffic demand of 1160 and 1161 veh/h, respectively, traveling from zone A to C. To avoid queuing at the connector leading to zone A, the link upstream of the top left ICA intersection is given unlimited stocking capacity. In this example, the subordinate assignment BFW is used in the ICA assignment. For the other two subordinate assignments, the same anomalies are observed.

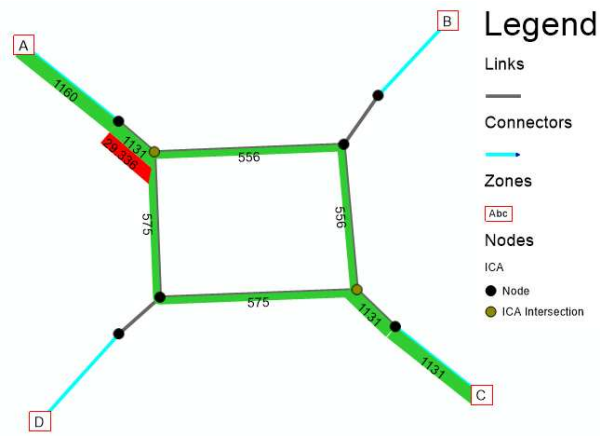

Figure 22: ICA assignment result with a traffic demand of 1160 veh/h

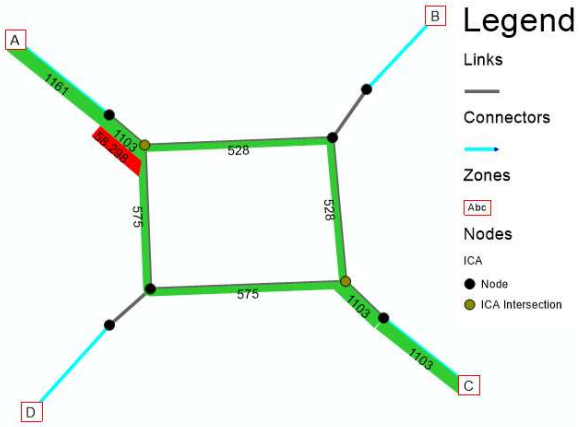

Figure 23: ICA assignment result with a traffic demand of 1161 veh/h

Although, the difference in demand is only 1 veh/h, the calculated traffic states are not as expected. Ideally, the scenario with a demand of 1161 veh/h should resemble the 1160 veh/h scenario, with the only difference being one extra vehicle traveling from zone A to C. Thus, the links included in the upper or lower route should count as one extra vehicle. However, the links in the upper route show an unexpected increase of 28 additional veh/h in the 1161 veh/h demand scenario compared to the 1160 veh/h demand. This difference demonstrates a minor piece of the oscillating pattern as seen in Figure 21.

The instability appearances are further confirmed with the determination of the stability measure for each demand scenario. The stability measures have a similar pattern as shown in Figure 21. In Figure 24, the average relative error (top) and maximum relative error (bottom) are shown for demand scenarios between 1000 veh/h and 2000 veh/h.

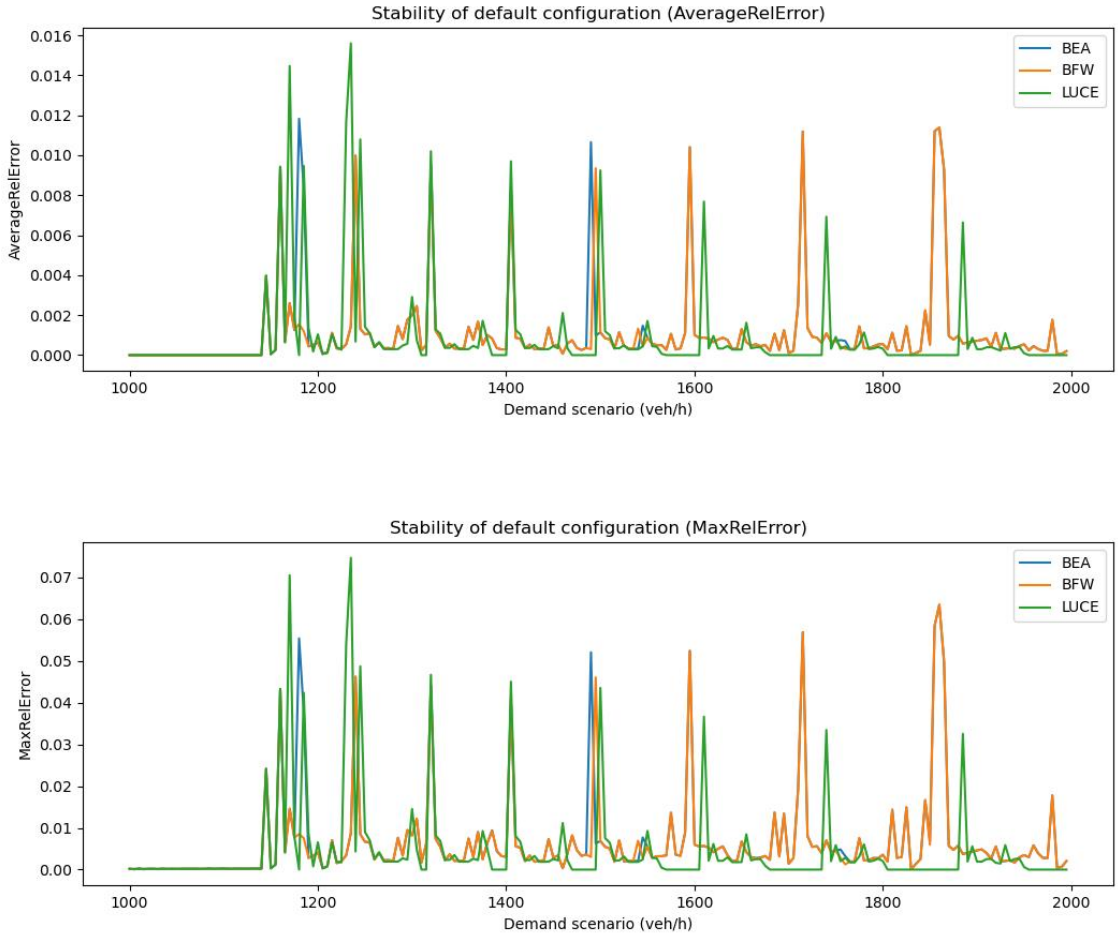

Figure 24: Stability analysis of ICA assignment in elementary network

Initially, the average relative- and max relative error are 0 since the volume differences in the network are equal to the expected routing of the perturbed demand. After a demand of roughly 1130 veh/h, relative errors show up in an oscillating pattern, much more defined compared to the total impedance in Figure 21. The graphs of BEA and BFW are almost identical and their relative error increases when more demand is allocated between zone A and C. On the other hand, the relative error of the LUCE algorithm is decreasing after starting with larger errors compared to BEA and BFW. With this, it can be concluded that instability occurs at least in the congested state, independent of the adopted subordinate assignment.

4.1.2 Convergence of the ICA assignment

The convergence of the ICA assignment is made up of six conditions as explained in the theoretical framework in section 2.2.5. The share for which each condition must be fulfilled is decisive in whether or not the ICA assignment will terminate. When one condition is not satisfied enough for its defined share percentage, the ICA assignment does not terminate even though the remaining shares are met. Based on the shared percentages that must be met, the convergence behavior for the demand interval is observed. In Figure 25, the convergence behavior of each subordinate assignment in the ICA assignment is shown. The traffic demand between zones A and C is plotted against the number of iterations. A single share graph follows the number of iterations that are needed until that share is satisfied.

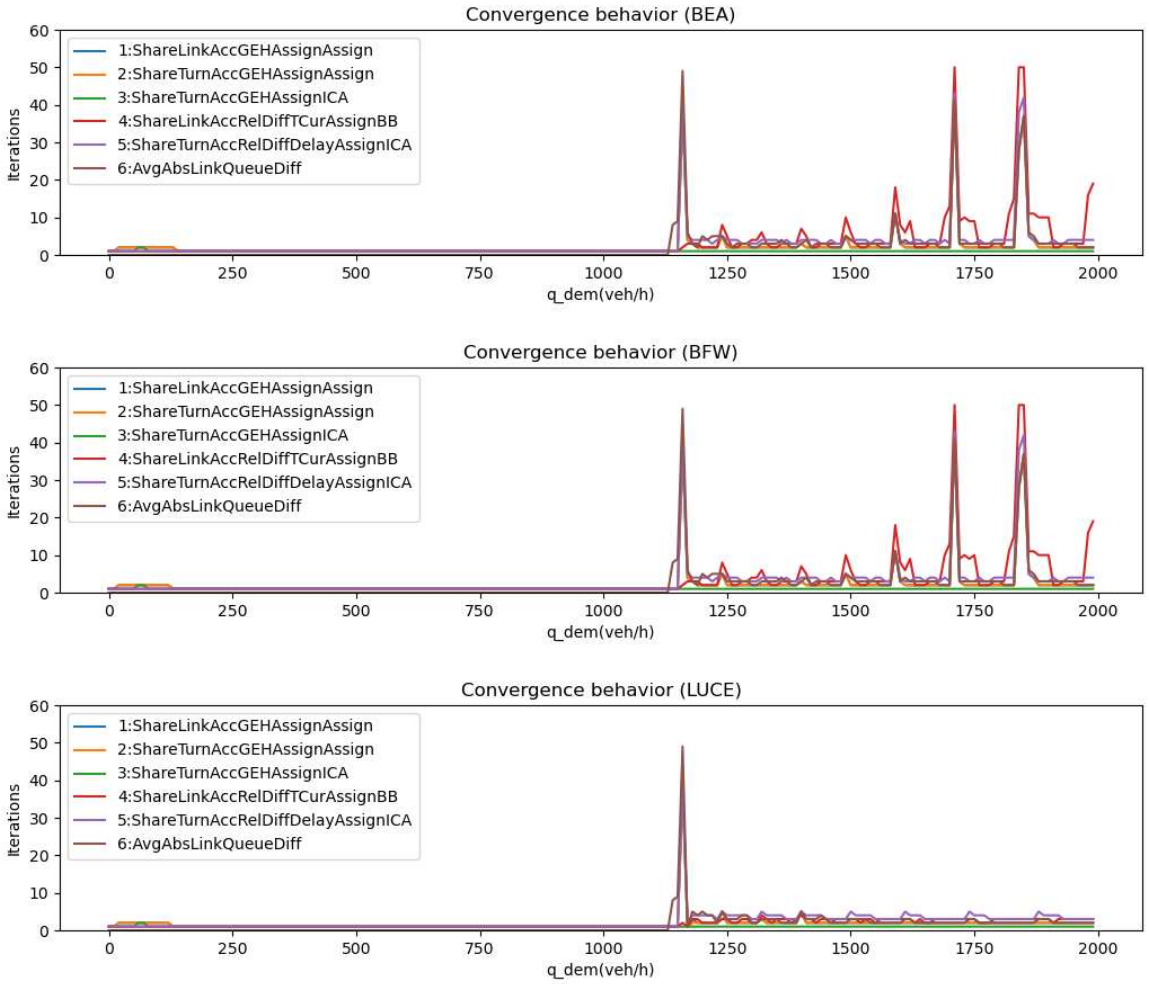

Figure 25: Convergence behavior of ICA assignment for three subordinate assignments

The graph shows that for all traffic demand scenarios lower than the capacity of the first ICA intersection, each share is fulfilled within a few iterations. After the near capacity threshold of 1130 veh/h, all subordinate assignments show a large peak for conditions 1, 2, 5, and 6. These are the differences between link volumes, turn volumes, turn delay, and link queues, respectively. From that moment, the condition shares require more iterations when the traffic demand increases. The ICA assignment with LUCE as subordinate assignment shows a different pattern than the BFW, which is nearly identical to the BEA graph. An ICA assignment with LUCE has a slight increase in iterations but keeps constant over the trajectory of demand. BFW and BEA require a continuously increasing number of iterations when the traffic demand grows. Moreover, the interval of these increasing number of iterations broadens as well.

A closer look at the convergence behavior for the BFW and BEA in the congested state shows that condition 6, the relative difference between VDF link travel time and blocking back calculated link travel time causes the slower convergence, depicted in red. Furthermore, conditions 1, 2, 5, and 6 pursue this same increasing pattern while condition 3 remains constant for all demand scenarios.

4.1.3 Impact input parameters

In section 3.6, the setup for the experiments has been explained which is conducted for both networks. In this section, the results of the experiments on the parameters in the elementary network are presented. In Figures 26 and 27, the average relative error and maximum relative error for all experiments are shown, where the subordinate assignments are distinguished by blue, orange, and green. Furthermore,

the relative and maximum relative error for the default settings are depicted with a dotted line, corresponding to its subordinate assignment.

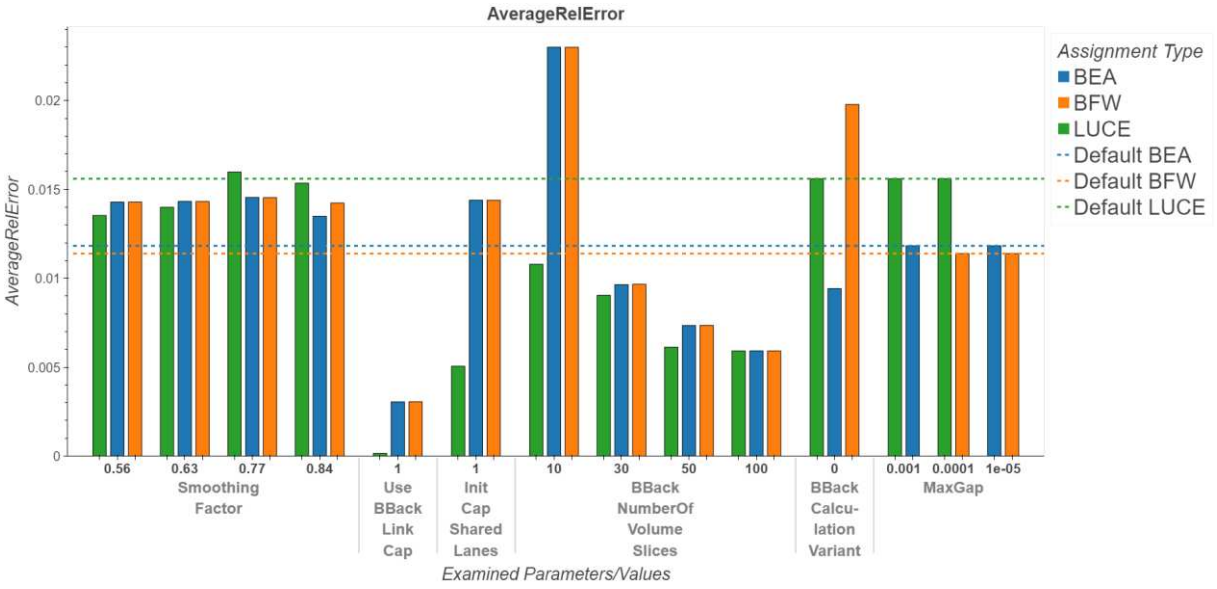

Figure 26: Average relative error of experiments in elementary network

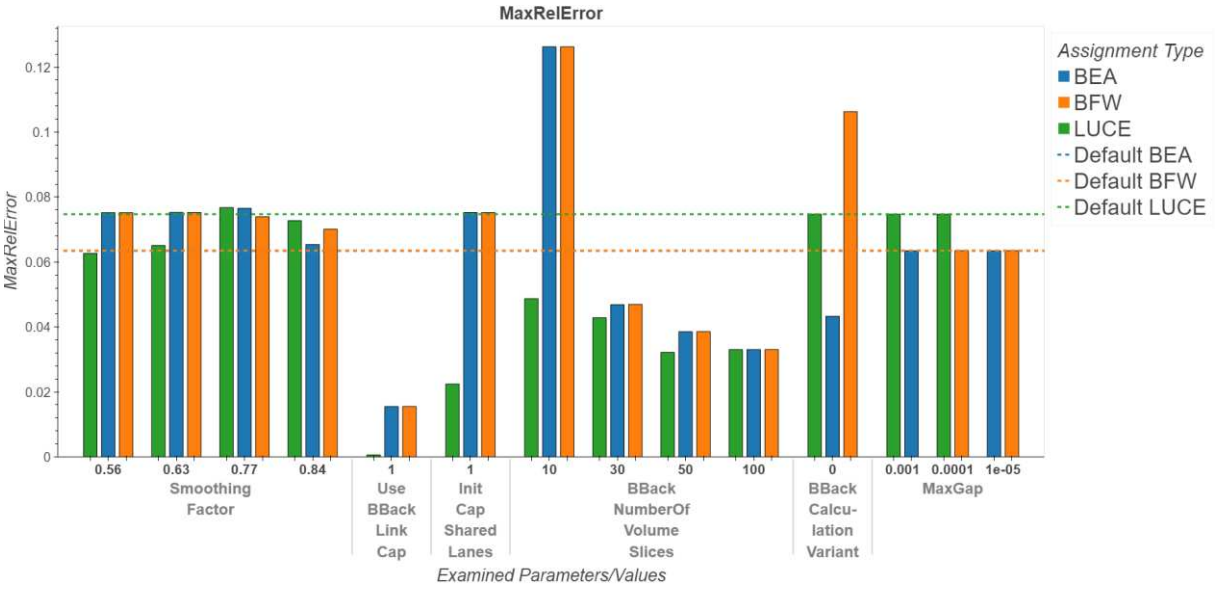

Figure 27: Maximum relative error of experiments in elementary network

At first, the ICA assignment with LUCE shows a significantly higher error for the default case compared to the BFW and BEA. Also, the results for BEA and BFW are very close to each other, which was observed in the default stability analyses as well.

Comparing the mutual result of subordinate assignments shows some remarkable outcomes. First, the LUCE algorithm contains a negligible error for the parameter "UseBBackLinkCap". The "InitCapSharedLanes" and a larger number of slices in "BBackNumerOfVolumeSlices" also slow a lower error compared to the default settings. The remaining parameters do not significantly differ from the default scenario. Regarding BEA, it is noticeable that the "UseBBackLinkCap" shows an improvement in stability as well. Although, the "InitCapSharedLanes" and 10 "BBackNumberOfVolumeSlices" are worse than the default scenario, whereas the other values for "BBackNumberOfVolumeSlices" show an improvement of stability. BFW has similar results as the BEA, except for the "BBackCalculationVariant". The "BBackCalculationVariant" has a negative

outcome on ICA assignment stability with BFW whereas BEA shows a relative error reduction. At last, the different values for MaxGap do not affect both errors and deliver the same result as the default experiment.

4.1.4 Discussion

In this chapter, the results of previous sections are discussed. First, the causes and consequences of the validated instability are addressed. Second, the outcome of the experiments is analyzed and the differences are explained. At last, the limitations and assumptions of the analysis carried out in an elementary network are summarized.

4.1.4.1 Instability of ICA assignment

The stability and convergence behavior of the default configuration follows a similar pattern in the case of using the BEA or BFW. A comparison of the convergence and the total volume in the network proves that there exists a correlation. Inspecting the behavior of these two instances in more detail shows the traffic volume drops at the moment the assignments need an extensive amount of iterations. In Figure 28, this is shown in more detail for scenarios between a demand of 1650 and 1750 veh/h, and a demand perturbation step of 1 veh/h.

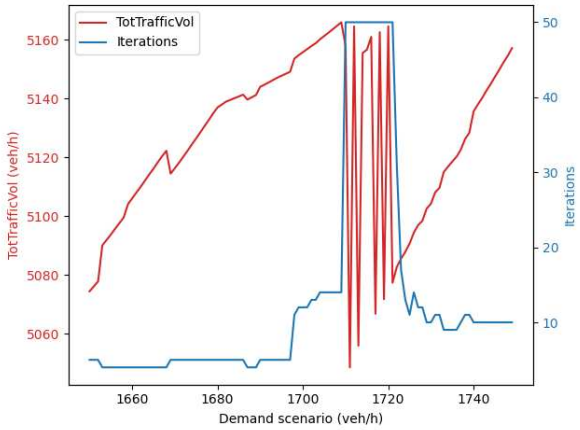

Figure 28: Detailed view of total traffic volume and number of iterations in the ICA assignment

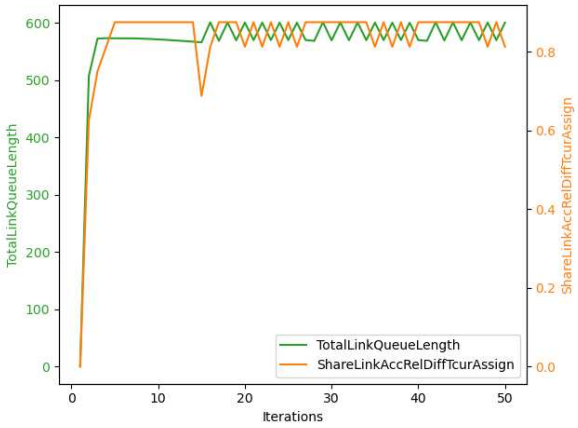

Figure 29: Detailed view of iteration results in the ICA assignment

It is visible that the ICA assignment switches between two calculated traffic volumes while the iterations reach out. When the iteration maximum is not considered, the ICA assignment will never converge at this point. Hence, the assignment is always prematurely ended to avoid extremely long computation times. The system does not converge because the relative difference between link VDF travel time and blocking back travel time is not met for a sufficient number of shares. Investigating the details of the iterations in the ICA assignment shows that the condition share for link travel time reaches a value that is slightly below the predetermined threshold of 90%. This has been worked out in Figure 29, where green is the total queue length on links and orange is the share value of the concerned iteration. At first, it seems that the assignment achieves convergence within a few iterations since the total queue length is almost constant at a value of 570 vehicles. However, the share for relative differences is not met, and the algorithm continues computing new solutions. As a result, the assignment computes two different traffic states and it alternates between the two from iteration to iteration. Because of the iteration limit of 50, an incorrect solution with a queue length of 600 is returned and is very different from the achieved result in the first 10 iterations. To overcome this, a possible strategy is to lower the minimum share to 85%. In this way, the algorithm will converge within a few iterations and return the expected solution.

The LUCE algorithm in the ICA assignment does not seem to have a relation between convergence and instability. The ICA assignment is always converging within a maximum of 10 iterations, while there is a clear presence of instability of high average relative errors for certain demand scenarios. A detailed investigation of the iterations of the ICA assignment has shown that the LUCE has a similar behavior

as the BEA and BFW. It fluctuates between two or more solutions that are significantly different. However, the assignment does compute the same solution twice instead of once in concurring iterations. This causes faster convergence for solutions that are not necessarily correct.

For each subordinate assignment, the ICA assignment is unstable due to the computation of multiple solutions for certain traffic demands. Therefore, the conservation of result uniqueness does not hold for each demand input.

4.1.4.2 Experiment results

Based on the results of the experiments, one could conclude that considering link capacities for the blocking back model with LUCE as subordinate assignment solves the problem of instability in the ICA assignment. It demonstrates to have an average error of almost zero. Hence, the perturbed demand is divided over the network according to the expected shortest paths. A reason that explains the stable LUCE result for using link capacities in the blocking back model is the unaffected calculations of delay at intersections. Because the capacity of the link upstream of the intersection is 1000 vehicles, it reaches capacity faster than the intersection itself. As a result, traffic will be blocked back earlier when link capacities are considered and the ICA procedures use an incoming traffic flow of 1000 for all scenarios with a demand greater than 1000. Similar reasoning can be used for the consideration of shared capacity instead of full capacity for the parameter "InitCapSharedLanes". Because the capacity of the shared turn is divided, the traffic is blocked back more regularly. Due to this, the queue is supplied with smaller doses of demand causing the system to converge more often towards the correct solution. Regarding the "BBackNumberOfVolumeSlices", higher values divide the traffic flow into more subsets. Hence, smaller numbers of traffic are blocked back each time such that the distribution is more evenly. This causes the queue to be approximated more accurately and the differences between solution alternatives in the ICA assignment will be smaller.

Among the other experiment results, there is no other parameter next to the "UseBBackLinkCap" that comes close to solving the problem of instability of the ICA assignment. In a previous section, it has been found that the ICA assignment often does not converge to a single solution but switches between two or more solutions. Regarding the BEA and BFW assignments, there are no parameter settings that bring the number of solutions to one for all demands. Moreover, there is a positive average relative error for all traffic demand that is allocated larger than the capacity of the first intersection. Some parameters such as the "InitCapSharedLanes", 10 slices for the "BBackNumberVolumeOfSlices", and BBackCalculationVariant enhance the effect of solution variation such that the differences become larger. This results in the additional average relative errors as shown in Figure 26.

4.1.4.3 Assumptions and limitations

First of all, the elementary network is a very minimal representation of larger networks. It has exclusively been developed to investigate the stability of the ICA assignment when two routes exist been an origin and destination zone. It could have been expanded with additional demand between the other zones. In this way, a more realistic situation would occur such that the outcome is of more practical worth.

With the stability results as presented in the default configuration, there is enough evidence to convey that instability of the ICA assignment is appearing in the elementary network. However, since it is an imaginary network the usability of these results must be criticized. Some elements in the network are very unlikely to happen in networks that are calibrated to real-world situations. At first, the network has been developed in such a way that heavy congestion effects occur. The scenarios that are developed allocate demand for up to 2000 vehicles. Hence, the queue that emerges because of the capacity constraint has a length of a maximum of 850 vehicles. Because queues with such lengths are never produced in traffic assignments considering congestion, the practicality of shown instability at this point is questionable. However, the results of average relative error in the default experiments show an immediate unstable scenario right after the capacity of the intersection was reached. This unstable

situation coincides with the sudden occurrence of a queue upstream of the overflowed intersection. At this exact moment, the convergence of the ICA assignment is reached much slower because of three conditions that cannot be met. Two of these consider queues that are not met for a sufficient number of shares. In other words, the ICA assignment is not able to accommodate the effects of queueing well in the procedure, such that convergence is reached in a few iterations.

4.2 Real-world network

In the real-world network, the same impact analysis of input parameters was conducted as for the elementary network. At first, the stability of the default configuration is investigated for the selected scenarios. In Figure 30, the stability results over the scenarios are shown. From top to bottom, the proportion of links that change, the average relative error, and the maximum relative error are shown, respectively. On the horizontal axis, the 20 selected scenarios are displayed based on their Euclidean distance between the perturbated OD pair.

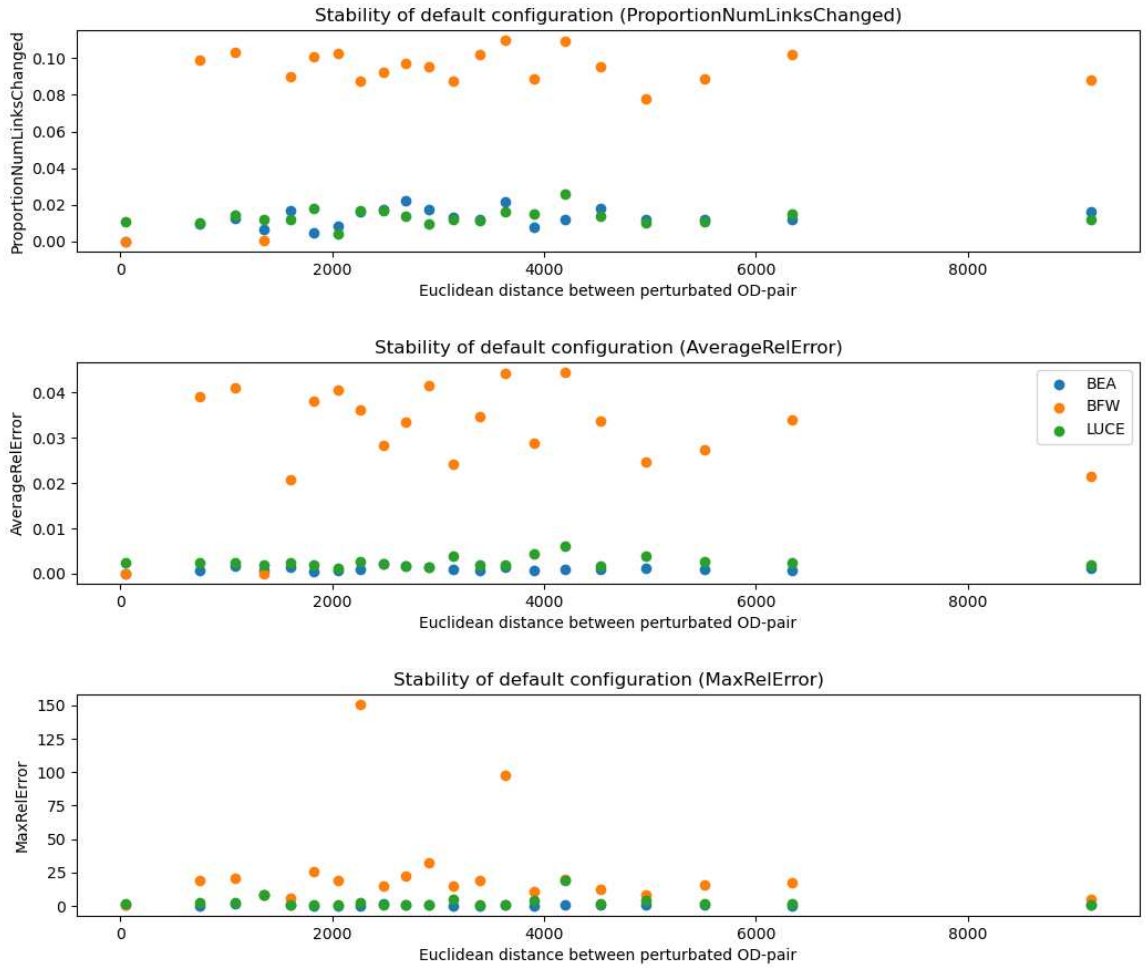

Figure 30: Stability of default configurations in real-world network

In all three stability measures can be seen that BFW is most unstable in the default configuration. With the use of the score table in Table 9, BFW's algorithm receives the lowest score for nearly all scenarios which have an average relative error of 0.01 an higher. Also, these scenarios present to have between 0.08 and 0.10 proportion of links changed. In other words, between 8% and 10% of the links in the network are changing with at least one vehicle, as a result of the perturbated demand. For the scenarios with an Euclidean distance of around 10 and 1500, the BFW is stable, with a relative error of approximately 0. Another observation is the difference between the graphs of maximum and average

relative error. For two scenarios with distances around 2200 and 3800, the maximum error is larger compared to the other instances.

The stability of BEA and LUCE is comparable and behaves more constantly over the scenarios than the BFW. Furthermore, their average relative error is between 0.000 and 0.005 for all scenarios, demonstrating to be more stable than BFW and score sufficient according to Table 9.

4.2.1 Impact input parameters

Besides the results of the default configuration, the experiments on the impact of parameters are executed. In Figures 31, 32, and 33, the experiment results are shown expressed in proportion of links, average relative error, and maximum relative error, respectively. For each experiment, the stability value is shown as an average of the 20 scenarios. The default configuration stabilities are depicted with the dotted lines and the subordinate assignments are distinguished by colors.

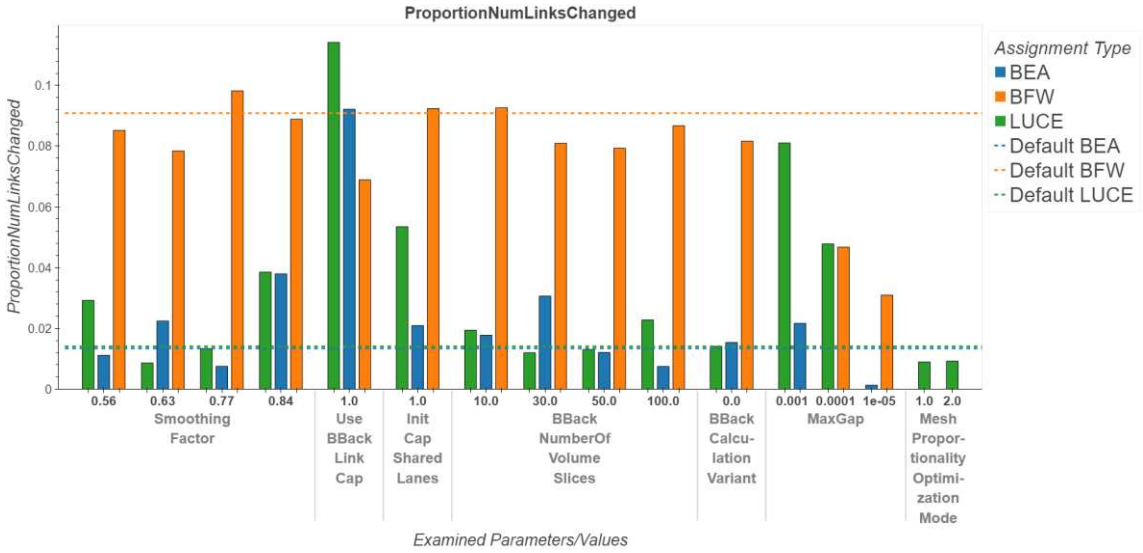

Figure 31: Experiment results (ProportionNumLinksChanged)

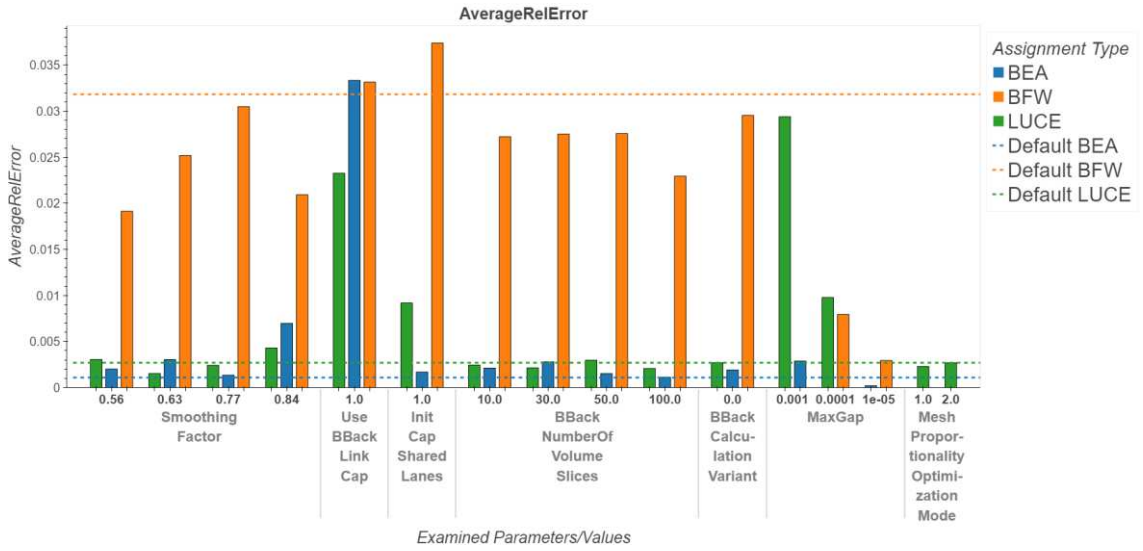

Figure 32: Experiment results (AverageRelError)

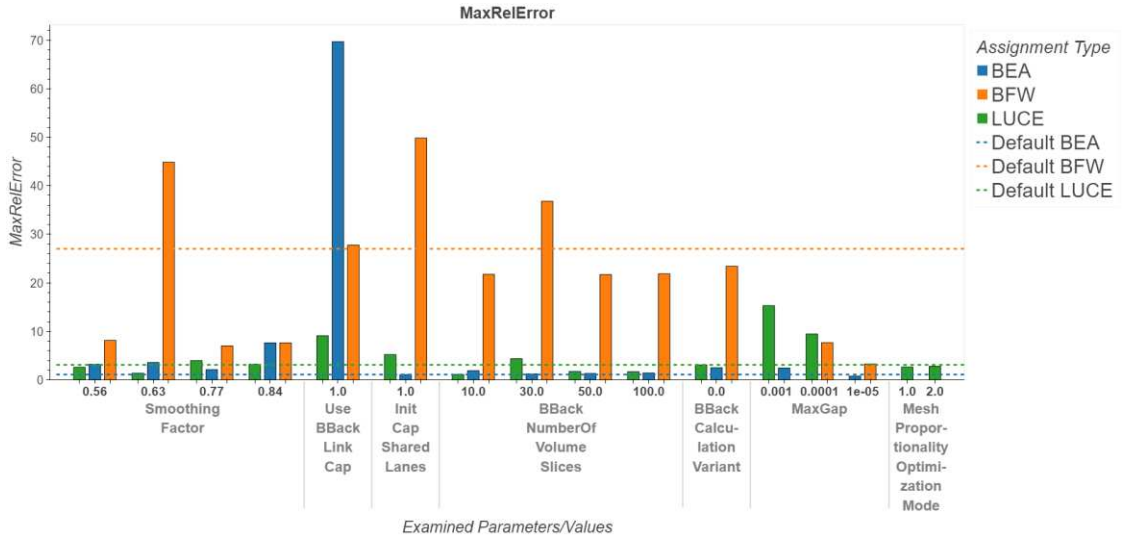

Figure 33: Experiment results (MaxRelError)

The experiment results show that the BFW has larger values for each stability measure than BEA and LUCE for the majority of experiments. Looking at the experiments expressed in average relative error in Figure 32, several anomalies stand out. First, the alternative BFW parameters have a positive impact on the average relative error except for the "UseBBackLinkCap" and "InitCapSharedLanes". However, for most parameters, the error reduction is not sufficient to reach a stable state such that the average relative error falls below 0.01. However, the "MaxGap" shows to be able to reduce the error to a rather stable state. With a "MaxGap" of 0.0001, the error has reduced by 4 times compared to a "MaxGap" of 0.001, the default configuration. When reducing the gap with another factor of 10, the error reaches a value of 0.003, which is considered relatively stable according to Table 9.

The "MaxGap" alternatives show similar results for BEA as well. The BEA shows a small increase in average relative error with a larger gap of 0.001 compared to its default configuration but complies with the same error as BFW at a gap of 0.00001. Furthermore, with a "MaxGap" in BEA of 0.00001, the average relative error is almost 0. For the LUCE assignment, the alternative "MaxGap" values have a higher average relative error compared to its default gap of 0.00001. Hence, it can be concluded that smaller maximum gaps in the subordinate assignment lead to an improvement of stability in the ICA assignment.

Next to the positive parameter impacts, some parameter settings have a significant negative impact on the stability. In contrast to the result of the experiments in the elementary network, the "UseBBackLinkCap" is not beneficial for the average relative error in BEA and LUCE. While BEA and LUCE conform to a stable default configuration, the "UseBBackLinkCap" is not able to ensure a stable outcome. Also the increased value of 0.84 in the "SmoothingFactor" and "InitCapSharedLanes" significantly worsen the average relative error of BEA and LUCE, respectively.

Regarding the maximum relative error, the results do not all follow the graph of average relative error in this case. A "SmoothingFactor" of 0.63 has a larger maximum relative error compared to the other alternative smoothing factors in the BFW assignment. Also, the default configuration has a maximum relative error higher than most of the "SmoothingFactor" alternative values. At last, the maximum relative error of UseBBackLinkCap has a different ratio between the three assignments compared to the average relative error. Especially, the BFW and LUCE maximum relative error is smaller than the BEA compared to the average relative error measure.

4.2.2 ICA Intersection configurations

In this section, the outcomes of single and multiple intersections calculated with ICA impacts on stability are presented. In Figure 34, the average relative error is shown in the network per intersection with ICA. Again, the intersections that are suitable and investigated in this analysis are indicated with circles.

Figure 34: Stability results of employing a single ICA intersection (subordinate assignment: BFW)

Based on the values of average relative error, a color is assigned to the intersection ranging from green to red. Hence, a green circle represents a stable network whereas a red circle is unstable. From the figure can be concluded that two intersections cause an unstable outcome when delays and capacities are calculated with the ICA procedure. Thus, an assignment with ICA including only a single ICA intersection is possible to return an unstable result.

The second analysis outcome holds the stability of the ICA assignment for different selected amounts of intersections with ICA. In Figure 35, the stability measures versus the possible number of intersections with ICA are shown.

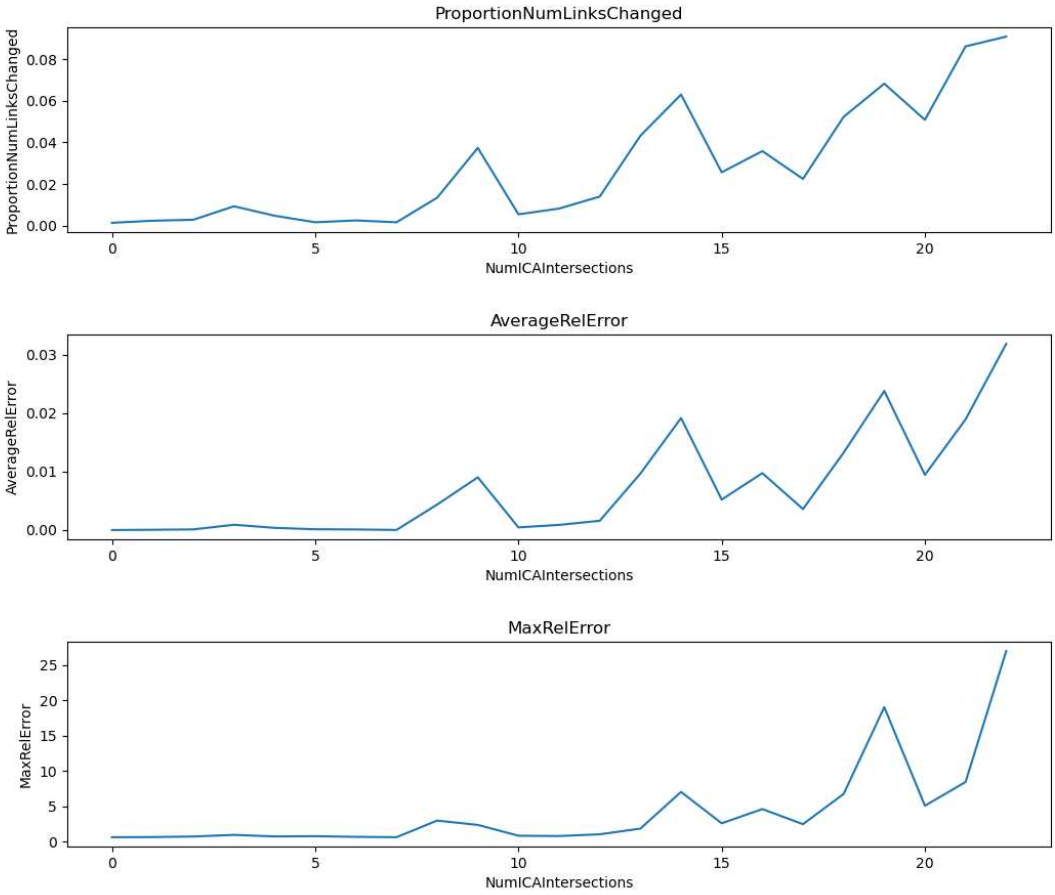

Figure 35: Stability results of different selected ICA intersections (subordinate assignment: BFW)

When more intersections are calculated with ICA, all stability measures increase on average. However, computing an additional intersection with ICA does not necessarily guarantee a less stable outcome. In each stability measure, the graph is increasing while fluctuating. In this case, the selection with 10 ICA intersections has an average relative error of 0.001, while the situation with 9 ICA intersections is unstable with an average relative error of almost 0.01. Thus, the number of intersections influences the state of stability in the ICA assignment. Nevertheless, it is possible to select up to 7 intersections such that the stability is preserved.

4.2.3 Discussion

In this section, the results of this research in the real-world network are discussed to highlight its practical and scientific benefits. Furthermore, the limitations and assumptions of the analysis in the real-world network are addressed.

4.2.3.1 Experiment results

The outcome of the experiments in the real-world network showed that the MaxGap has the most impact on the stability of all subordinate assignments in the ICA assignment. When considering the same gap for all three assignments, the BEA scores the best, followed by LUCE and BFW. With a smaller maximum gap, the subordinate assignments find a more accurate solution, since the differences between their successive iterations are smaller. This could explain the improved stability of a smaller MaxGap in the ICA assignment. More accurate subordinate assignment solutions, narrow the chance of deviating outcomes between iterations in the ICA assignment However, some further discussion of these results is needed before concluding ranking BEA on top. Since all three assignments are different their effectivity might depend on the considered environment.

The quality of the equilibrium is a major performance indicator for its scientific benefits. An important measure for a good equilibrium is the achievement of Wardrop's first principle. This states that all drivers cannot reduce their travel time by unilaterally changing routes (Wardrop, 1952). In other words, the travel cost or impedance of 2 or more routes between the same OD-pair must be equal and any other route choice is more costly. In Table 12, the impedance difference between concurring routes as the ratio of the total impedance is shown. Furthermore, all alternative routes created between the same OD-pairs are given. This has been computed for all subordinate assignments at three different maximum gaps.

Table 12: Equilibrium performance of subordinate assignments (default configuration)

Subordinate assignment	Parameter	Value	Impedance difference ratio	Alternative routes created
BEA	MaxGap	0.001	0.000138	170
		0.0001	0.000166	236
		0.00001	0.000185	264
BFW	MaxGap	0.001	0.010476	26803
		0.0001	0.021472	31207
		0.00001	0.026779	61782
LUCE	MaxGap	0.001	0.002497	8501
		0.0001	0.004487	9138
		0.00001	0.007315	10273

The table shows that a smaller gap yields more alternative routes for each subordinate assignment. For BFW, this effect is the largest such that 61782 alternative routes exist for a maximum gap of 0.00001. When a subordinate assignment is bounded to a smaller gap, it is encouraged to find more alternative routes such that the objective function is optimized. However, a smaller maximum gap does not lead to a better succession of the Wardrop first principle. Each subordinate assignment cannot entirely meet the requirements of Wardrop's statement that competing routes have equal impedance. The ideal case should return an impedance difference ratio of 0. Thus, BEA meets the Wardrop condition best, with LUCE second and BFW third. However, the BEA result offers a substantially less amount of alternative routes compared to the BFW and LUCE. Given the fact that there are 70756 OD-pairs in the network, BEA assumes that almost all traffic chooses the same route to get to their destination. On the other hand, the BFW suggests that for nearly all OD-pairs 2 possible routes exist on average, at a gap of 0.00001. This delivers a much more complex solution, which has more chances of deviating from Wardrop's first principle. Furthermore, the increased complexity of the BFW could account for its instability relative to the BEA and LUCE. The incorporation of more routes in the solution allows for greater fluctuations. However, the experiment result concluded that a smaller gap leads to more stability, which goes against this statement. As this research only considered link flows, this hypothesis remains unconfirmed.

4.2.3.2 ICA intersection locations

The intersections suitable for the ICA assignment are located at different places in the network. Based on the outcome of running a stability analysis for single intersections calculated with ICA, 2 turned out to be unstable while the others were not. Since each intersection has different geometry and characteristics, these could influence the stability. However, an examination of the characteristics did not find any elements that connect these intersections to the instability result. Therefore, the outcome of the ICA assignment is investigated in more detail. This has resulted in a remarkable change in queue length over the network for the unstable intersections. In Figure 36, the queuing in the network is shown when carrying out an ICA assignment with all suitable ICA intersections calculated with the ICA. The traffic flows as a result of the assignment are depicted with green bars, and queueing is shown in red bars. The length of the queue around each intersection is summarized with the number in the boxes in meters.

Figure 36: Outcome of the ICA assignment (subordinate assignment: BFW)

In the network, queueing effects are happening around the intersections causing an unstable situation. Hence, it can be concluded that the queueing at intersections is primarily responsible for the instability of the ICA assignment. This has also been observed in the stability analyses in the elementary network and can be confirmed with these results.

The ICA assignment has been developed to include delays at intersections in traffic assignment results. Since congestion at intersections contributes to the maximum occurrence of delay, these effects need to be captured. It is worrying that the ICA assignment is unable to yield successful outcomes at locations where it is most effective.

4.2.3.3 Limitations and assumptions

One major asset of this research is the real-world network which has been built by counting and calibration. Due to this, fewer assumptions were necessary. Still, an assumption has been made for the impedance perceived by travelers. In this study, travelers decide to make a trip based on travel time and travel distance only. In reality, many more aspects play a role in deciding on a trip and this depends majorly on the destination characteristics.

Furthermore, the real-world network is part of a larger network that has been used for the calibration. Therefore, the calibrated values will not entirely match the situation of the considered network in this research. In Visum, it is possible to obtain a smaller piece of a network by defining sub-boundaries. However, observation showed that identical configurations of ICA assignments do not provide the same results for the calibrated network and the real-world network as part of the original network. This is a minor limitation of the real-world approach since the calibrated values in the real-world network do not perfectly match its original.

Another limitation is the restricted parameter values that were tested. The experiments were focused on a selected set of parameters that seemed likely to impact model stability based on preliminary analysis

and theoretical framework. However, more parameters could have been investigated and influence the stability of the ICA assignment.

Until now, the ICA assignment is only implemented in the Visum software. This restricts its application for external projects. Since Visum is a costly enterprise, only a limited number of people can use it within their transport modeling practices.

The current stability measure considers link flows only. Hence, it is missing the response of route flows to the perturbations. When comparing two situations that have an equal stability result based on link flows might not return the same stability for route flows. It is possible that in one scenario, the link flows are concentrated along a few longer routes, whereas in other scenarios, they are distributed across a variety of different shorter routes.

5 Conclusion and recommendations

This research aimed to explore the instability issues in the ICA assignment when integrated with user equilibrium traffic assignments using the Visum software. The study focused on identifying the impact of various parameters on the stability of the model and finding the causes of instability to give recommendations for improved stability in the ICA assignment. This objective has been captured with the following proposed research question: "How can the current state of instability appearing in the Intersection Capacity Analysis combined with a user equilibrium traffic assignment be alleviated?"

5.1 Summary and key findings

The current state of instability in the ICA assignment has been validated through a case study in an elementary network. This network contains minimal attributes such that demand flows between two zones and travels two optional routes. Both routes travel along two intersections where delays and capacities are calculated with the ICA. The instability is observed by comparing a selection of 200 different demand sizes between the two zones. The ICA assignment demonstrates instability primarily when traffic demand exceeds the capacity of the first encountered intersection. In these scenarios, the traffic state predictions downstream of this intersection vary while it is expected to stay unchanged since no traffic can pass. Furthermore, the instability is characterized by fluctuations between multiple traffic volume outcomes without reaching convergence.

To determine how various input parameters impact the stability of the ICA assignment, a series of systematic experiments were designed and executed. These experiments were applied to both the elementary network and a real-world network. Each parameter was varied individually to assess its impact while keeping all other parameters constant at their default settings. This approach ensured that any observed changes in model stability could be attributed directly to the parameter being tested. For each parameter setting, the corresponding stability is computed. The stability is measured with an assessment framework. In this framework, stability was quantified using two primary indices: the average relative error and the maximum relative error. These indices were calculated for each parameter setting, providing a detailed measure of how the traffic volumes on links were affected by the changes in parameters.

The outcome of the experiments in the elementary network showed that the consideration of link capacities in "UseBBackLinkCap" had a significant positive impact on the stability for all three subordinate assignments. Furthermore, the use of the shared capacity for shared lanes in "InitCapSharedLanes" and higher values for "BBackNumberOfVolumeSlices" did improve the stability as well. On the other hand, the parameters of the blocking back model for BFW and BEA, the use of shared capacities at shared lanes "InitCapSharedLanes", the distribution of traffic volume in 10 slices in "BBackNumberOfVolumeSlices" and the method of capacity exploitation "BBackCalculationVariant", all negatively impact the stability. In the real-world network, the experiment results are different compared to the elementary network. Here, the "MaxGap" has the largest positive impact, whereas the "UseBBackLinkCap" parameter has a strong negative impact on stability.

The configuration and number of intersections analyzed using ICA within the model have an impact on the stability as well. Examining the location of intersections suitable for ICA in the real-world network showed that two intersections cause instability. Comparing this with the result of the ICA assignment showed that the intersections causing instability are congested such that queueing occurs. Hence, the congestion effects have an impact on the stability, as also observed in the stability analysis in the elementary network. Situations, where more intersections are analyzed with the ICA, tend to exhibit more instability on average, suggesting that each additional intersection calculated with ICA enhances the chance of retrieving an unstable result.

Overall, an ICA assignment with BEA and LUCE as subordinate assignments has been found more stable than using BFW. Reducing the "MaxGap", which refers to the convergence threshold in the subordinate assignments, was found to significantly improve the stability of the model. Eventually, the BEA provided with a maximum gap of 0.00001 proves to give the best stability of the ICA assignment while also maintaining the equilibrium criteria according to Wardrop's principle. However, the BEA equilibrium details are minimalistic. It solves the equilibrium with hardly any alternative routes between identical OD pairs, whereas the BFW delivers a rather complex equilibrium. This complex equilibrium is a better representation of reality. Therefore, a trade-off must be made when choosing a subordinate assignment for the ICA assignment between accuracy and stability.

5.2 Recommendations for further research

Because of the limited research on the combination of equilibrium assignments and the ICA, multiple directions of further research are suggested. There is a need for the development of robust algorithms within traffic modeling tools next to Visum that can more effectively handle scenarios of high traffic demand and congestion. Additionally, efforts should be made to integrate the ICA assignment into more accessible or open-source traffic modeling platforms to broaden their application.

This research has only been focused on the ICA for signalized intersections. For a further direction, it is valuable to consider the ICA assignment stability when the ICA is applied to other intersection control types. Moreover, more research is suggested on the influence of the detailed ICA procedure itself on the stability of the ICA assignment. In this research, the components in the ICA have not been examined as part of the parameter impact on the ICA assignment stability.

Regarding the definition of stability, only link flows are considered in this research. It can be expanded by incorporating the effects of routing as well. This would provide a more comprehensive understanding of traffic behaviors and help in refining the traffic models. Furthermore, the quality of subordinate assignments has been briefly examined. A further direction can be to conduct more research into the routes determined in subordinate assignments as part of the ICA assignment and connect this with the stability of route- or link flows.

Only three different subordinate assignments are considered in this research. Based on the results, the subordinate assignments have a significant impact the instability. Therefore, it is valuable to execute research into more different subordinate assignment types in the ICA assignment. However, either a careful Visum implementation of them is necessary or an external ICA assignment must be realized before this research can be done.

At last, the outcome of this research has proven that queuing effects are the root cause of instability in the ICA assignment. More research is suggested into the relationship between the blocking back model and the instability. As long as the ICA assignment is unable to perform stable results at congested areas, it should not be used here. Furthermore, the process of VDF parameter adjustment and modification is performed such that the convergence of a solution should be maintained. Parameter adjustments during calculations is uncommon in traffic assignments because it violates the separability rules of unique equilibria. Therefore, more research should be done to the influence of VDF parameter adjustments and instability.

6 Bibliography

Akcelik, R. (1981). *Traffic signals: capacity and timing analysis* (Research Report ARR No. 123 (7th reprint: 1998) ed.). Melbourne: Australian Road Research Board.

Bar-Gera, H. (2002). Origin-based algorithm for the traffic assignment problem. *Transporation Science, 36*(4), 398-417.

Bar-Gera, H. (2010). Traffic assignment by paired alternative segments. *Transportation Research Part B: Methodological, 44*(8-9), 1022-1046.

Beckman et al. (1956). *Studies in the economics of transportation.* New Haven: Yale University Press.

Boyce et al. (2010). *Field Test of a Method for Finding Consistent Route Flows and Multiple-Class Link Flows in Road Traffic Assignments: Prepared for: Federal Highway Administration.* US Federal Highway Administration.

Boyce, D., Ralevic-Dekic, B., & Bar-Gera, H. (2004). Convergence of traffic assignments: how much is enough? *Journal of Transportation Engineering, 130*(1), 49--55.

BPR. (1964). *Traffic Assignment Manual.* Washington DC: Urban planning division, US Department of Commerce.

CBS. (2023). *Inwoners per gemeente*. Retrieved from DashboardBevolking: https://www.cbs.nl/nl-nl/visualisaties/dashboard-bevolking/regionaal/inwoners

CROW. (2015). *Basiskenmerken kruispunten en rotondes* (Vol. 1). CROW. Retrieved from https://www.crow.nl/publicaties/basiskenmerken-kruispunten-en-rotondes

Dafermos, S., & Sparrow, F. . (1969, February 18). The Traffic Assignment Problem for a General Network. *JOURNAL OF RESEARCH of the National Bureau of Standards - B. Mathematical Sciences, 73B*(2), 91-118.

Dial, R. B. (2006). A path-based user-equilibrium traffic assignment algorithm that obviates path storage and enumeration. *Transportation Research Part B: Methodological, 40*(10), 917-936.

Federal Highway Administration. (2023). *Manual on Uniform Traffic Control Devices for Streets and Highways.* U.S. Department of Transportation.

Gentile, G. (2014). Local user cost equilibrium: a bush-based algorithm for traffic assignment. *Transportmetrica A: Transport Science, 10*(1), 15-54.

Google. (2024). *Utrecht*. Retrieved April 8, 2024, from https://www.google.com/maps/@52.1038019,5.1206905,429m/data=!3m1!1e3?entry=ttu

Hillier, J. A., & Rothery, R. (1967). The synchronization of traffic signals for minimum delay. *Transportation Science, 2*(1), 81-94.

Jayakrishnan et al. (1994). *A Faster Path-Based Algorithm for Traffic Assignment.* Berkeley, California: The University of California Transportation Center.

Jin, W.-L. (2008). On the stability of user equilibria in static transportation networks. *Transportmetrica, 4*(1), 1-17.

Lu, S., & Nie, Y. M. (2010). Stability of user-equilibrium route flow solutions for the traffic assignment problem. *Transportation Research Part B: Methodological, 44*(4), 609-617.

Mitradjieva, M., & Lindberg, P. O. (2013). The stiff is moving—Conjugate direction Frank-Wolfe methods with applications to traffic assignment. *Transportation Science, 47*(2), 280-293.

National Highway Traffic Safety Administration (NHTSA). (2003). *A Compilation of Motor Vehicle Crash Data from the Fatality Analysis Reporting System and the General Estimates System.* USDOT. Washington, DC: Traffic Safety Facts 2002. Retrieved from Traffic Safety Facts 2002.

National Research Council (U.S.). Transportation Research Board. (2022). *Highway capacity manual : a guide for multimodal mobility analysis (Seventh edition).* National Academies Press. doi:https://doi.org/10.17226/26432

Nie, Y. M. (2010). Equilibrium analysis of macroscopic traffic oscillations. *Transportation Research Part B: Methodological, 44*(1), 62-72.

Ortúzar, J. d., & Willumsen, L. (2011). *Modeling Transport 4th Edition.* Chichester, West Sussex, United Kingdom: John Wiley & Sons.

Patil et al. (2021). Convergence behavior for traffic assignment characterization metrics. *Transportmetrica A: Transport Science, 17*(4), 1244-1271.

Patriksson, M. (2015). *The traffic assignment problem: models and methods.* Courier Dover Publications.

Perederieieva et al. (2013). A computational study of traffic assignment algorithms. *Australasian Transport Research Forum*, *1C*, p. 2.

Planung Transport Verkehr GmbH. (2024). *The world's leading transport planning software*. Opgehaald van PTV Group: https://www.ptvgroup.com/en/products/ptv-visum

PTV Group. (2023). *PTV Visum manual.* Karlsruhe: PTV Plannung Transport Verkehr GmbH.

Robertson, D. I. (1979). *Traffic Models and Optimum Strategies of Control: A Review.* Berkeley: Transport and Road Research Laboratory.

Sawar, S., Sipos, T., Bilal, M. T., & Verebélyi, B. (2021). Exploring Correlation between Highway Intersection Capacity and Traffic Parameters. *Periodica Polytechnica Transportation Engineering, 49*(4), 344-353.

Sheffi, Y. (1985). *Urban transportation networks* (Vol. 6). Englewood Cliffs, NJ: Prentice-Hall.

Smith, M. J. (1979). The existence, uniqueness and stability of traffic equilibria. *Transportation Research Part B: Methodological, 13*(4), 295-304.

Transportation Research Board of the National Academies. (1985). *Highway Capacity Manual.* Washington, D.C.: National Research Council.

TRB. (2016). *The highway capacity manual 6th edition: A guide for multimodal mobility analysis.* Washington, D.C.: The National Academies of Sciences, Engineering and Medicine.

Wardrop, J. G. (1952). Road paper. some theoretical aspects of road traffic research. *Proceedings of the institution of civil engineers, 1*(3), 325-362.

Webster, F. V. (1958). *Traffic signal settings.* Road Research Laboratory. London: HMSO.

Xie, J., & Nie, Y. (2019). A new algorithm for achieving proportionality in user equilibrium traffic assignment. *Transportation Science, 53*(2), 566-584.

7 Appendix

7.1 Appendix A: Bi-Conjugate Frank Wolfe

Determine starting point $\boldsymbol{x_0}$ such that $f(\boldsymbol{x_0})$

At iteration $\boldsymbol{k}$:

1. Determine the first Taylor expansion of the function $f(\boldsymbol{x})$.

$$f_k(\boldsymbol{x}) = f(\boldsymbol{x_k}) + \nabla f(\boldsymbol{x_k})^T(\boldsymbol{x} - \boldsymbol{x_k}) \quad (70)$$

2. Compute the **search direction** by calculating the minimizer y_k^{FW} that minimizes $f_k(\boldsymbol{x})$

$$y_k^{FW} = min(\nabla f(\boldsymbol{x_k})^T \boldsymbol{x}) \quad (71)$$

Then, the search direction is given by

$$d_{\boldsymbol{k}}^{FW} = y_k^{FW} - \boldsymbol{x_k} \quad (72)$$

3. If $\boldsymbol{k} = 0{,}1\ or\ \gamma_{\boldsymbol{k-1},\gamma_{\boldsymbol{k-2}}} = 1$, $d_{\boldsymbol{k}}^{BFW} = d_{\boldsymbol{k}}^{FW}$. Else

$$d_{\boldsymbol{k}}^{BFW} = \beta_{\boldsymbol{k}}^0 d_{\boldsymbol{k}}^{FW} + \beta_{\boldsymbol{k}}^1 \left(s_{\boldsymbol{k-1}}^{BFW} - \boldsymbol{x_k}\right) + \beta_{\boldsymbol{k}}^2 \left(s_{\boldsymbol{k-2}}^{BFW} - \boldsymbol{x_k}\right) \quad (73)$$

Here $\beta_{\boldsymbol{k}}^0, \beta_{\boldsymbol{k}}^1, \beta_{\boldsymbol{k}}^2$ are defined by

$$\beta_{\boldsymbol{k}}^0 = \frac{1}{1 + \mu_{\boldsymbol{k}} + v_{\boldsymbol{k}}} \quad (74)$$

$$v_{\boldsymbol{k}} = \frac{(s_{\boldsymbol{k-1}} - \boldsymbol{x_k})^T H(\boldsymbol{x_k}) d_{\boldsymbol{k}}^{FW}}{(s_{\boldsymbol{k-1}} - \boldsymbol{x_k})^T H(\boldsymbol{x_k})(s_{\boldsymbol{k-1}} - \boldsymbol{x_k})} + \frac{\mu_{\boldsymbol{k}} \gamma_{\boldsymbol{k-1}}}{1 - \gamma_{\boldsymbol{k-1}}} \quad (75)$$

$$\mu_{\boldsymbol{k}} = \frac{(\gamma_{\boldsymbol{k-1}} s_{\boldsymbol{k-1}} - \boldsymbol{x_k} + (1 - \gamma_{\boldsymbol{k-1}}) s_{\boldsymbol{k-2}})^T H(\boldsymbol{x_k}) d_{\boldsymbol{k}}^{FW}}{(\gamma_{\boldsymbol{k-1}} s_{\boldsymbol{k-1}} - \boldsymbol{x_k} + (1 - \gamma_{\boldsymbol{k-1}}) s_{\boldsymbol{k-2}})^T H(\boldsymbol{x_k})(s_{\boldsymbol{k-2}} - s_{\boldsymbol{k-1}})} \quad (76)$$

$$\beta_{\boldsymbol{k}}^1 = v_{\boldsymbol{k}} \beta_{\boldsymbol{k}}^0 \quad (77)$$

$$\beta_{\boldsymbol{k}}^2 = \mu_{\boldsymbol{k}} \beta_{\boldsymbol{k}}^0 \quad (78)$$

4. Find the **step size** by a **line search**. Minimize the objective $f\left(\boldsymbol{x_k} + \gamma_{\boldsymbol{k}} d_{\boldsymbol{k}}^{CFW}\right)$

$$\gamma_{\boldsymbol{k}} = argmin(f\left(\boldsymbol{x_k} + \gamma_{\boldsymbol{k}} d_{\boldsymbol{k}}^{CFW}\right) \quad (79)$$

5. Calculate the new points with

$$\boldsymbol{x_{k+1}} = \boldsymbol{x_k} + \gamma_{\boldsymbol{k}} d_{\boldsymbol{k}}^{FW} \quad (80)$$

7.2 Appendix B: Adjustment factors

7.2.1 Adjustment factor for lane width (f_w)

The adjustment for lane width penalties the saturation flow rate in case of narrow lanes and increases the actual saturation flow rate for wider lanes. Based on the lane width, the factor's value is determined in Table 13.

Table 13: Lane width adjustment factors

Average lane width (m)	**Adjustment factor (f_w)**
<3.048	0.96
>=3.048-3.9319	1.00
>3.9319	1.04

7.2.2 Adjustment factor for lane utilization (f_{LU})

In situations of movement groups having more than one exclusive or shared lane, the lane utilization adjustment factor accounts for this. The factor is determined by

$$f_{LU} = \frac{v_g}{v_{gl} * N} \tag{81}$$

Where v_g is the unadjusted volume of lane group g and v_{gl} the highest unadjusted volume of lane l in lane group g.

7.2.3 Adjustment factor for right turns (f_{RT})

When a turn is subjected to a right turn, an adjustment factor is used. Depending on the type of lane, the adjustment factor is established as shown in Table 14 for single lanes, exclusive lanes, and shared lanes, respectively.

Table 14: Right-turn adjustment factors

Single lane	$f_{RT} = 1.0 - (0.135)P_{RT}$
Exclusive lane	$f_{RT} = 0.85$
Shared lane	$f_{RT} = 1.0 - (0.15)P_{RT}$

Where, P_{RT} is the proportion of vehicles turning right.

7.2.4 Adjustment factor for left turns (f_{LT})

Similarly, for right turns, the left turns in the ICA have an adjustment factor as well. However, left turns are influenced by more elements than right turns. An example is signalized intersections with permissive phasing. These enable certain movement groups to conflict under clear rules. In the case of protected phasing, all lane groups do not have to worry about conflicting with other lanes when receiving green. For the protected phasing, the adjustment factors are determined shown in Table 15.

Table 15: Left-turn adjustment factors for protected phasing

Exclusive lane	$f_{LT} = 0.95$
Shared lane	$f_{LT} = \frac{1}{1.0 + 0.05P_{LT}}$

Where P_{LT} is the proportion of vehicles turning left.

For a signalized intersection with permitted phasing, the adjustment factor is determined as follows:

$$f_{LT} = \left(\frac{g_u}{g}\right) * \left(\frac{1}{1 + P_L * (E_{L1} - 1)}\right) \quad 82$$

$$P_L = 1 + \frac{(N-1) * g}{\frac{g_u}{E_{L1} + 4.24}} \quad 83$$

$$g_u = \begin{cases} g - g_q \; if \; g_q \geq 0 \\ g \; else \end{cases} \quad 84$$

$$g_q = v_{olc} * \frac{qr_0}{0.5 - \left[v_{olc} * \frac{1 - qr_0}{g_0}\right]} - t_l \quad 85$$

$$v_{olc} = \frac{v_o * C}{3600 * N_o * f_{LU_o}} \quad 86$$

An explanation of the notations is given in table 16 below.

Table 16: Parameters in left-turn adjustment factor

Parameter	Description
g	Effective non-protected green time for left-turn lane group
g_u	Effective non-protected green time for left-turns crossing a conflicting flow
g_q	Effective non-protected green time, while left-turns are blocked completely
g_o	Effective green time for conflicting lanes o
P_L	Proportion of left-turns using lane L in shared lane
E_{L1}	Through equivalent for non-protected left-turns
N	Number of lanes
v_{olc}	Flow for conflicted lanes o corrected per lane l per cycle c
N_o	Number of lanes of conflicting flow o
v_o	Corrected conflicting flow o
f_{LU_o}	Lane utilization adjustment factor for conflicting flow o
qr_o	Queue ratio of conflicting flow o
t_l	Loss time of left-turning lane l

7.3 Appendix C: Mean delays per lane group

The total delay is composed of the uniform delay, incremental delay, and initial queue delay. Moreover, the uniform delay is multiplied by a progression factor PF.

7.3.1 Uniform delay

The uniform delay is delay measured at a uniformly distributed arrival rate. This delay is calculated as

$$d_1 = 0.5 * C * \frac{\left(1 - \frac{g}{C}\right)^2}{1 - \min\left(1, \frac{v}{c}\right)\frac{g}{C}} \quad 87$$

Where all variables are defined in Table 3. The progression factor PF_1 is determined by a complex formula as given in equation 88.

$$PF_1 = \frac{1 - P}{1 - \frac{g}{C}} * \frac{1 - y}{1 - \min\left(1, \frac{v}{c}\right)P} * \left(1 + \min\left(1, \frac{v}{c}\right) * \frac{g}{C} * \left(\frac{1 - P * \frac{C}{g}}{1 - \frac{g}{C}}\right)\right) \quad 88$$

Where :

PF: the progression factor
P: proportion of vehicles arriving during green

The other variables are defined in Table 3.

7.3.2 Incremental delay

The incremental delay accounts for the delay due to random arrivals next to the uniform arrivals. This is calculated by

$$d_2 = 900T * (\left(\frac{v}{c}\right) - 1 + \sqrt{\left(\frac{v}{c} - 1\right)^2 + \frac{8kI\frac{v}{c}}{cT}} \quad 89$$

Where:

T: the duration of the analysis period
k: incremental delay factor
I: the upstream filtering adjustment factor

The other variables are defined in Table 3.

7.3.3 Initial queue delay

The initial queue delay is added when a queue exists at the beginning of the analysis period. This is calculated as follows:

$$d_3 = \frac{1800 * Q_{queue} * (1 + u) * t}{cT} \quad 90$$

Where:

u: a delay parameter
t: duration of queue as part of T
T: the duration of the analysis period

The other variables are defined in Table 3.

7.4 Appendix D: Queue lengths

The mean queue length is determined by queues in uniform and random arrivals. The queue at uniform arrivals is multiplied by a progression factor PF_2.

7.4.1 Uniform queue length

The uniform queue length accounts for the number of vehicles that arrive at a red stage or at a green stage when there is a queue already. This is calculated as

$$Q_1 = PF_2 * \frac{\frac{v * C}{3600} * (1 - \frac{g}{C})}{1 - \left(min1, \frac{v}{c}\right)\frac{g}{C}} \quad 91$$

The progression factor is calculated with

$$PF_2 = \frac{\left(1 - R_p * \frac{g}{C}\right) * 1 - \frac{v}{s}}{\left(1 - \frac{g}{C}\right) * \left(1 - R_p * \frac{v}{s}\right)} \quad 92$$

All variables are defined in Table 3.

7.4.2 Incremental queue length

The incremental queue length represents the number of vehicles that arrive at random. This is calculated as follows:

$$Q_2 = 0.25cT * \left(\left(\frac{v}{c} - 1\right) + \frac{Q_{queue}}{cT} + \sqrt{\left(\frac{v}{c} + 1 + \frac{Q_{queue}}{cT}\right)^2 + \frac{8 * k * \frac{v}{c}}{cT} + \frac{16 * k * Q_{queue}}{cT^2}} \right) \quad 93$$

Where

k: incremental delay factor
T: the duration of the analysis period

The other variables are defined in Table 3.

7.5 Appendix E: Convergence conditions settings for ICA assignment

Table 17: Convergence criteria

Condition	Name	Description	Max value	Min share
1	ShareLinkAccGEHAssignAssign	Difference between traffic link volumes between consecutive iterations	1	95%
2	ShareTurnAccGEHAssignAssign	Difference between traffic turn volumes between consecutive iterations	1	95%

3	ShareTurnAccGEHAssignICA	Difference between traffic turn volume and smoothed turn volumes	1	95%
4	ShareLinkAccRelDiffTCurAssignBB	Difference in VDF link delay and blocking back model delay	0.05	90%
5	ShareTurnAccRelDiffDelayAssignICA	Difference between VDF turn delay and ICA turn delay	0.05	90%
6	AvgAbsLinkQueueDiff	Difference between queue lengths in consecutive iterations	1	-

7.6 Appendix F: Parameter settings for ICA assignment analysis in elementary network

Table 18: Default parameter settings ICA assignment

Phase	**Parameter**	**Value**
Subordinate assignment	Type	BFW
	MaxGap	0.001
	MaxIterations	200
Blocking back model	Calculation variant	Capacity exploited evenly over all routes
	Considered capacity	Turns
	Number of shares for flow distribution	20
	Average space required per car unit	7 meters
Initial occupancy	Saturation flow rate of turns	1900 veh/h/lane
	The initial capacity of lanes at shared lanes	Total capacity for each turn
Other	Minimum capacity of turns	10 veh/h
	Scaling factor	1
	Maximum iterations of ICA assignment	50
	Smoothing factor	0.7